Experimental, Computational, Theoretical and Analytical Investigation of Flow Boiling in Reduced Gravity

V.S. Devahdhanush, Jeongmin Lee, Steven Darges, Issam Mudawar

Purdue University Boiling & Two-Phase Flow Laboratory (PU-BTPFL)
School of Mechanical Engineering
585 Purdue Mall
West Lafayette, IN 47907

Tel. (765) 494-5705
Email: mudawar@ecn.purdue.edu

Mohammad M. Hasan, Henry K. Nahra, R. Balasubramaniam, Rochelle L. May

NASA Glenn Research Center
21000 Brookpark Road
Cleveland, OH 44135

Jeffrey R. Mackey

HX5, LLC
3000 Aerospace Parkway,
Brook Park, OH 44142

November 3-6, 2021

Experimental Investigation: Mission Sequence Testing

Two-phase Flow Loop

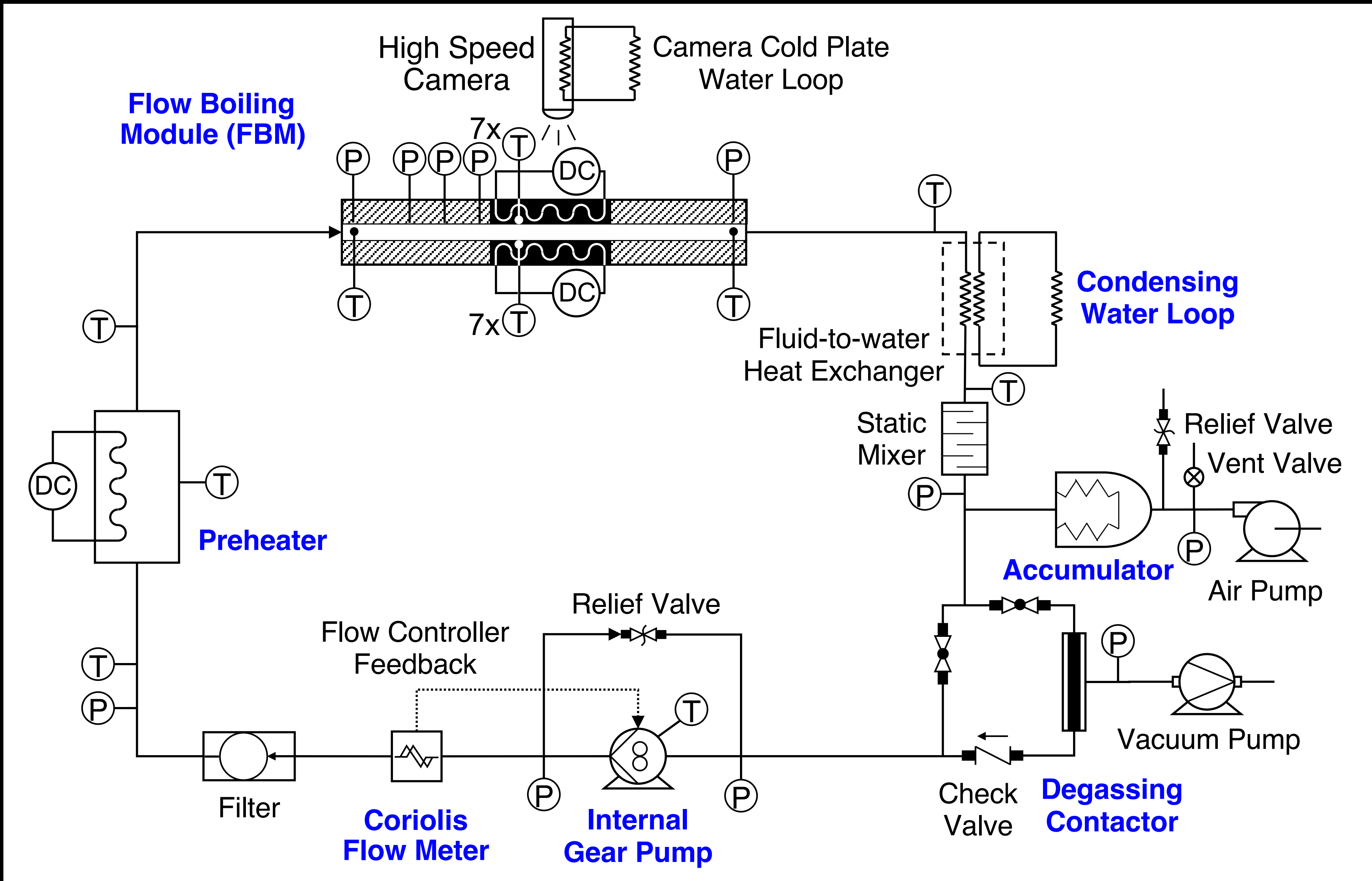

PURDUE UNIVERSITY

Flow Boiling Module (FBM)

NASA

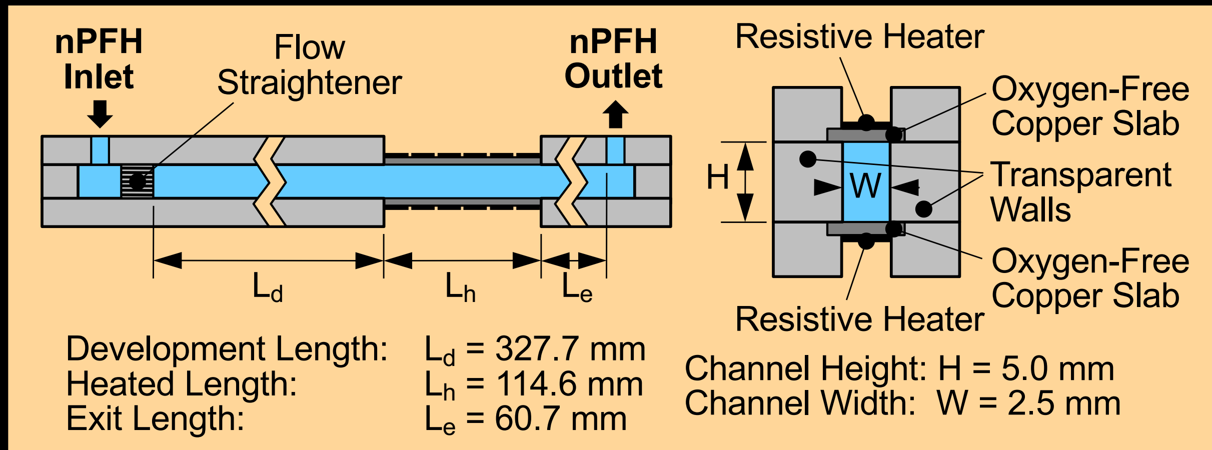

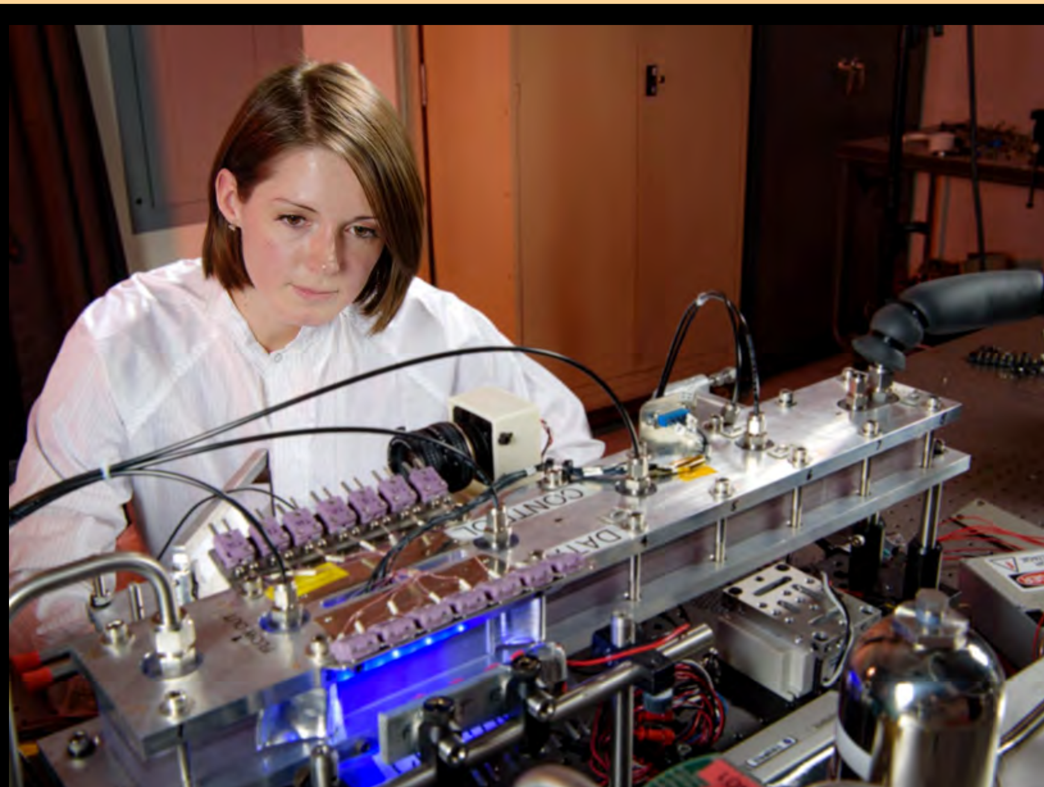

Temporal Variation of Wall Temperatures for Heat Flux Increments from 0 to CHF

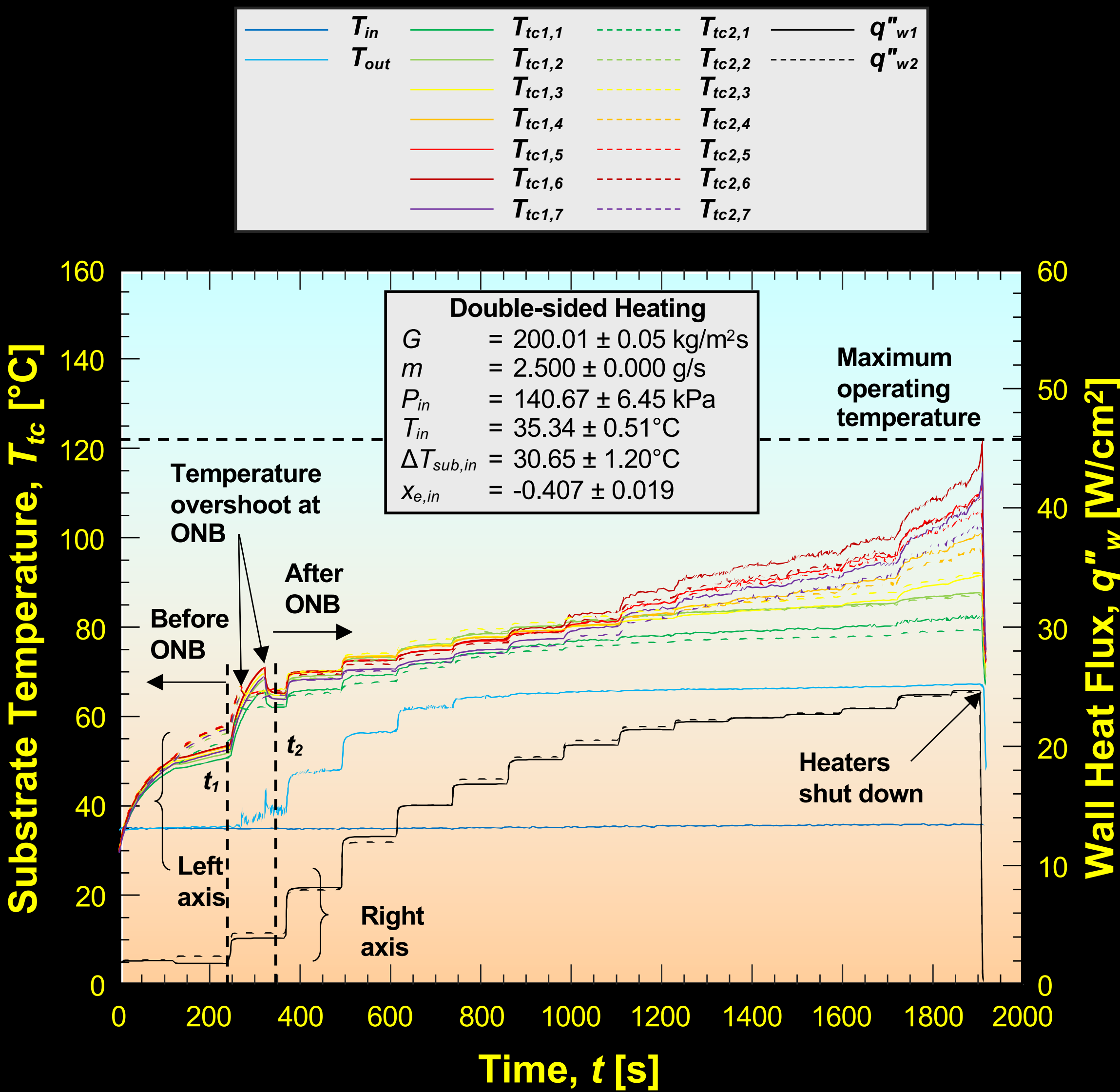

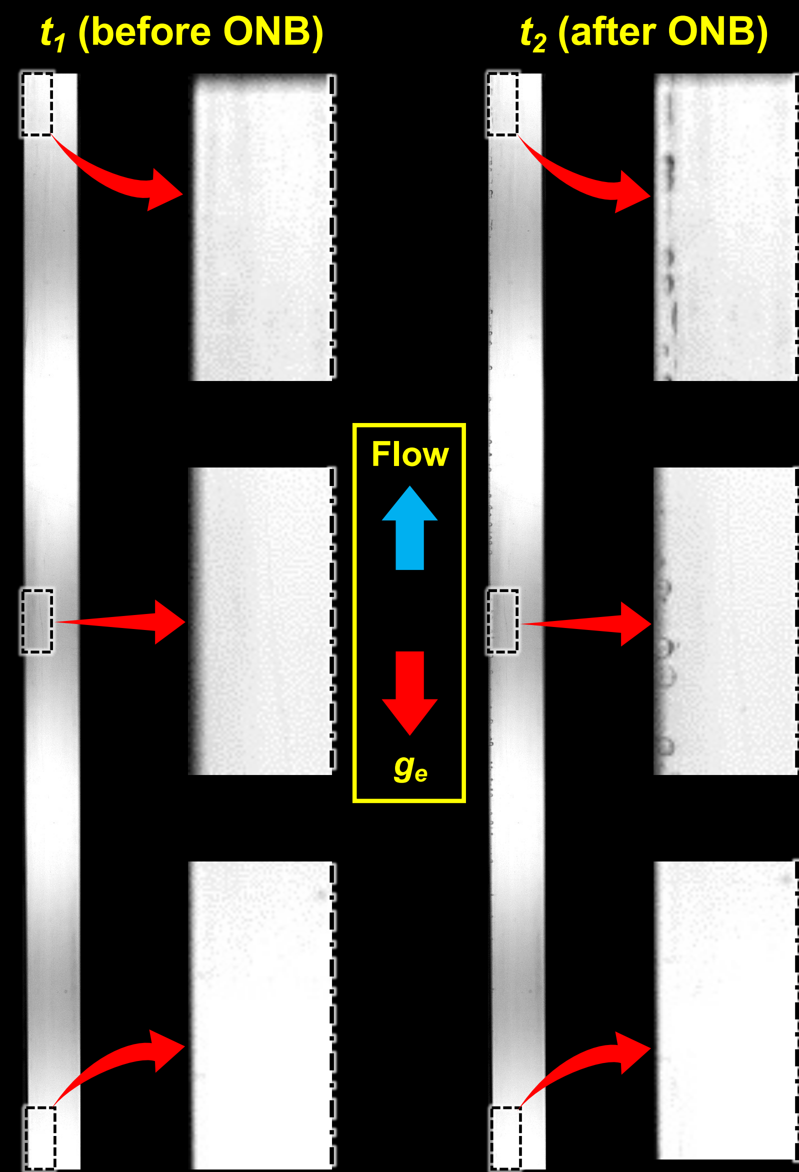

Flow Patterns along Boiling Curve – Highly Subcooled Inlet

Double-sided Heating

G = 200.01 kg/m²s, p_{in} = 135.62 kPa
T_{in} = 35.34°C, $\Delta T_{sub,in}$ = 30.65°C, $x_{e,in}$ = -0.407
q''_{CHF1} = 24.52 W/cm², q''_{CHF2} = 24.39 W/cm²

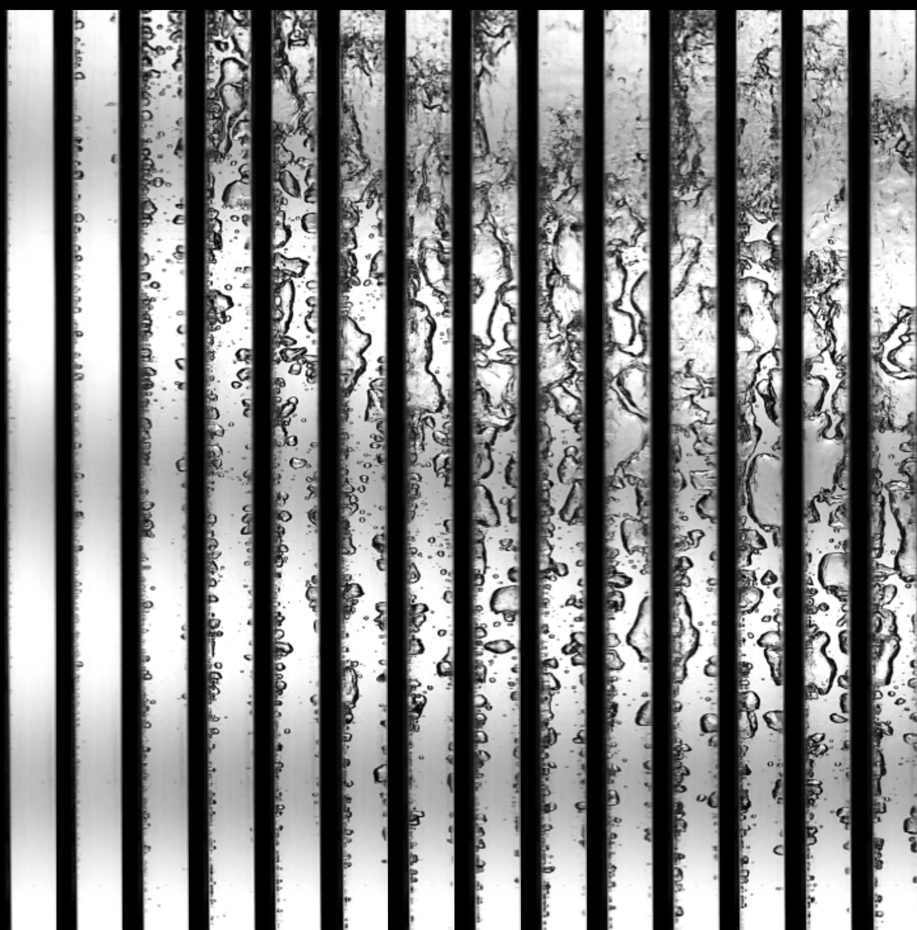

q''_w (% q''_{CHF}): 16.91%, 32.99%, 49.88%, 61.61%, 69.74%, 77.71%, 83.10%, 88.03%, 90.61%, 91.66%, 93.00%, 94.78%, 99.28%, 100.0%

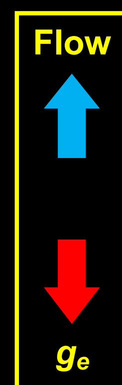

G = 1599.94 kg/m²s, p_{in} = 124.06 kPa
T_{in} = 35.75°C, $\Delta T_{sub,in}$ = 27.49°C, $x_{e,in}$ = -0.361
q''_{CHF1} = 43.21 W/cm², q''_{CHF2} = 43.94 W/cm²

q''_w (% q''_{CHF}): 27.94%, 36.83%, 44.65%, 55.69%, 67.99%, 80.09%, 83.20%, 91.47%, 100.0%

Flow Patterns along Boiling Curve – Near-Saturated Inlet

PURDUE UNIVERSITY

Double-sided Heating

G = 199.98 kg/m²s, p_{in} = 132.19 kPa
T_{in} = 62.61°C, $\Delta T_{sub,in}$ = 2.60°C, $x_{e,in}$ = -0.035
q''_{CHF1} = 16.68 W/cm², q''_{CHF2} = 16.72 W/cm²

G = 3199.97 kg/m²s, p_{in} = 143.63 kPa
T_{in} = 59.51°C, $\Delta T_{sub,in}$ = 8.29°C, $x_{e,in}$ = -0.113
q''_{CHF1} = 43.13 W/cm², q''_{CHF2} = 43.07 W/cm²

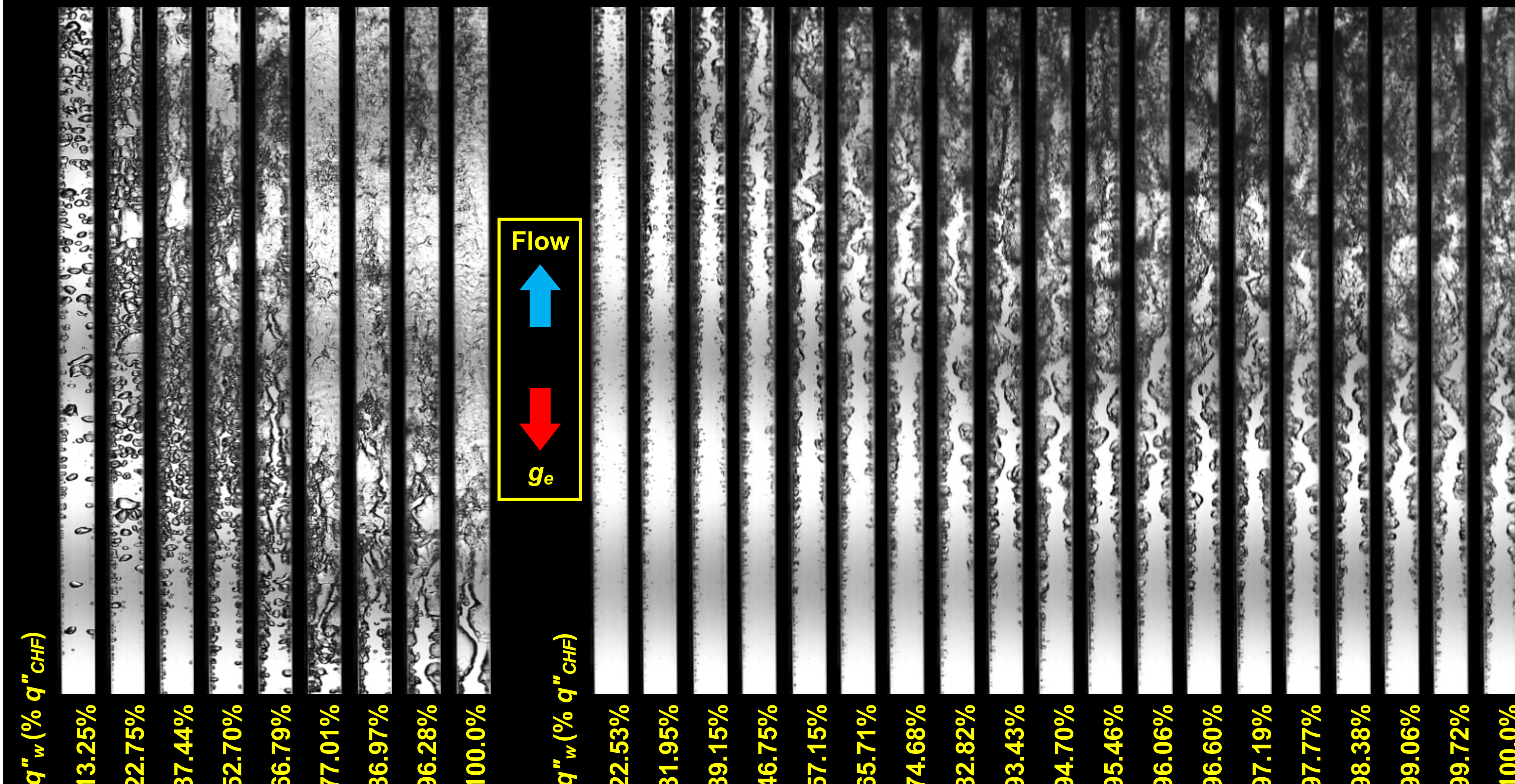

Boiling Curves for Different Heating Configurations

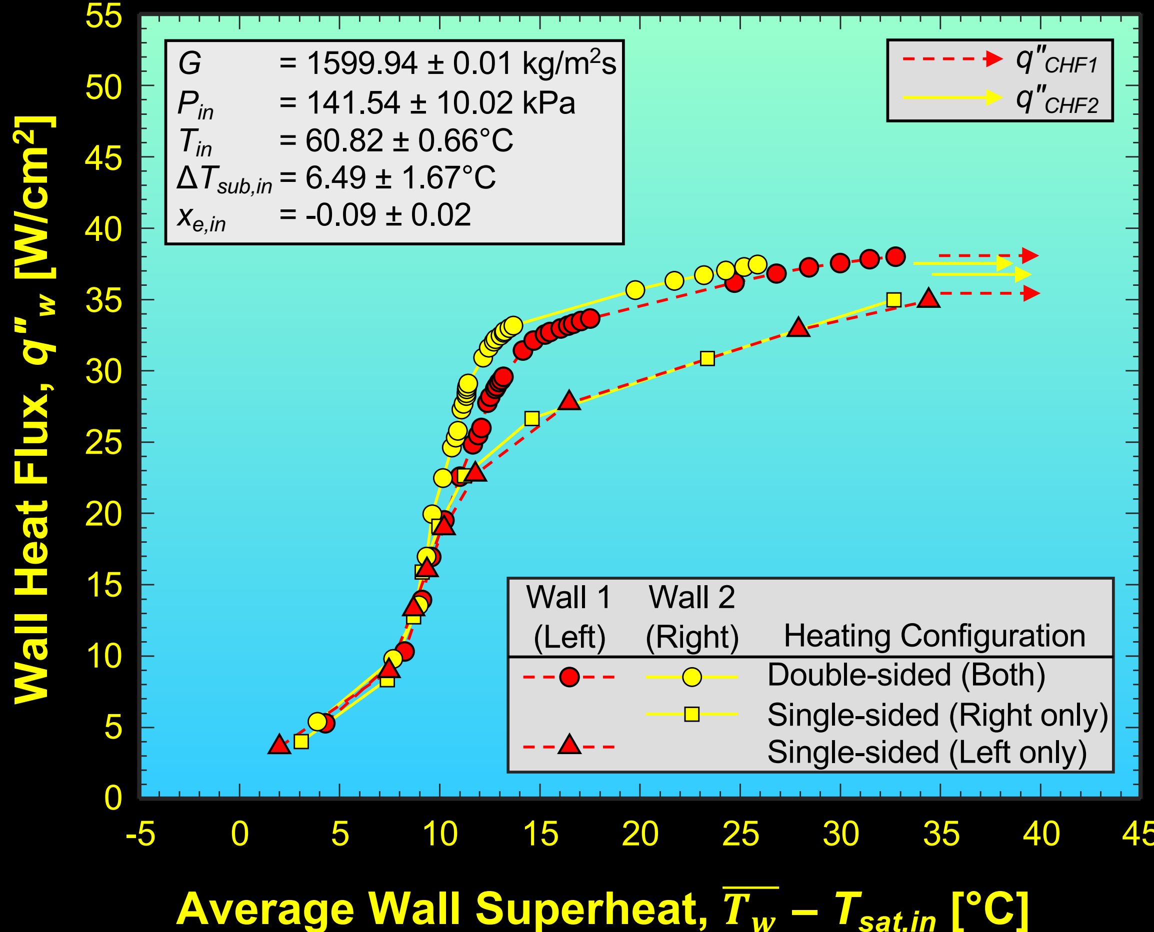

Effects of Mass Velocity and Fluid Inlet Subcooling

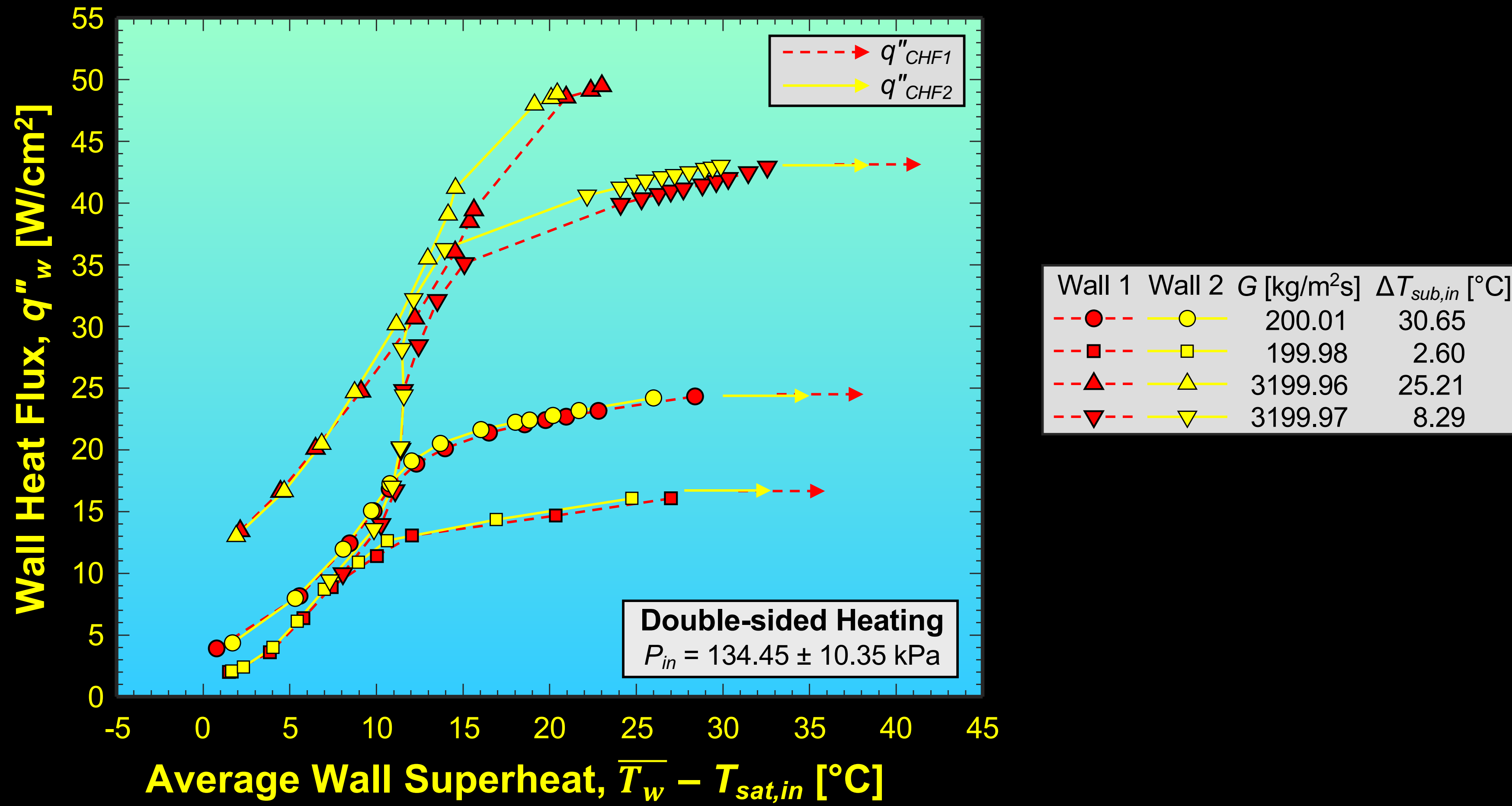

Axial Variations of Wall Temperature

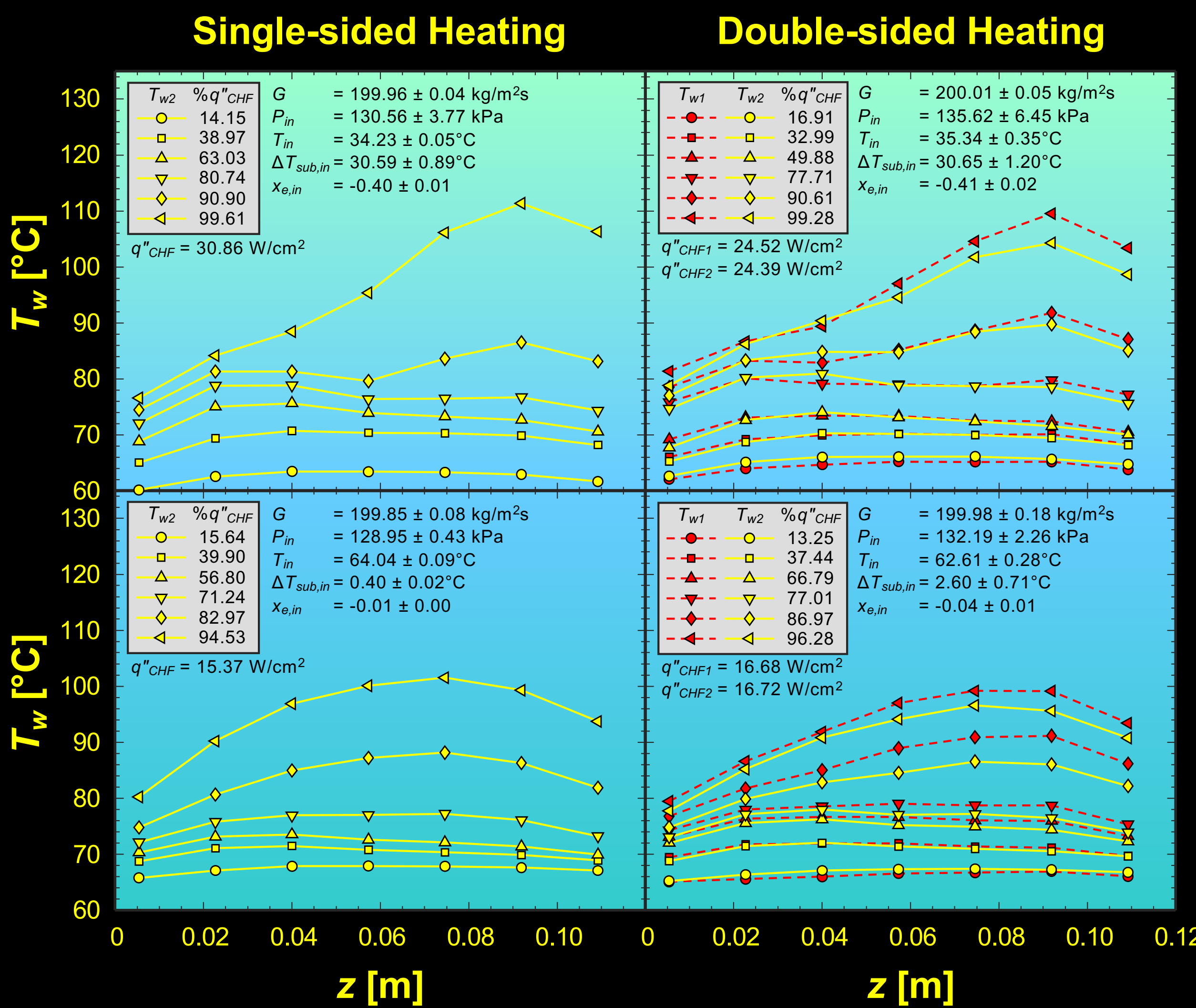

Low Mass Velocity
Highly Subcooled
Low Inlet Pressure

Low Mass Velocity
Near Saturated
Low Inlet Pressure

Axial Variations of Heat Transfer Coefficient

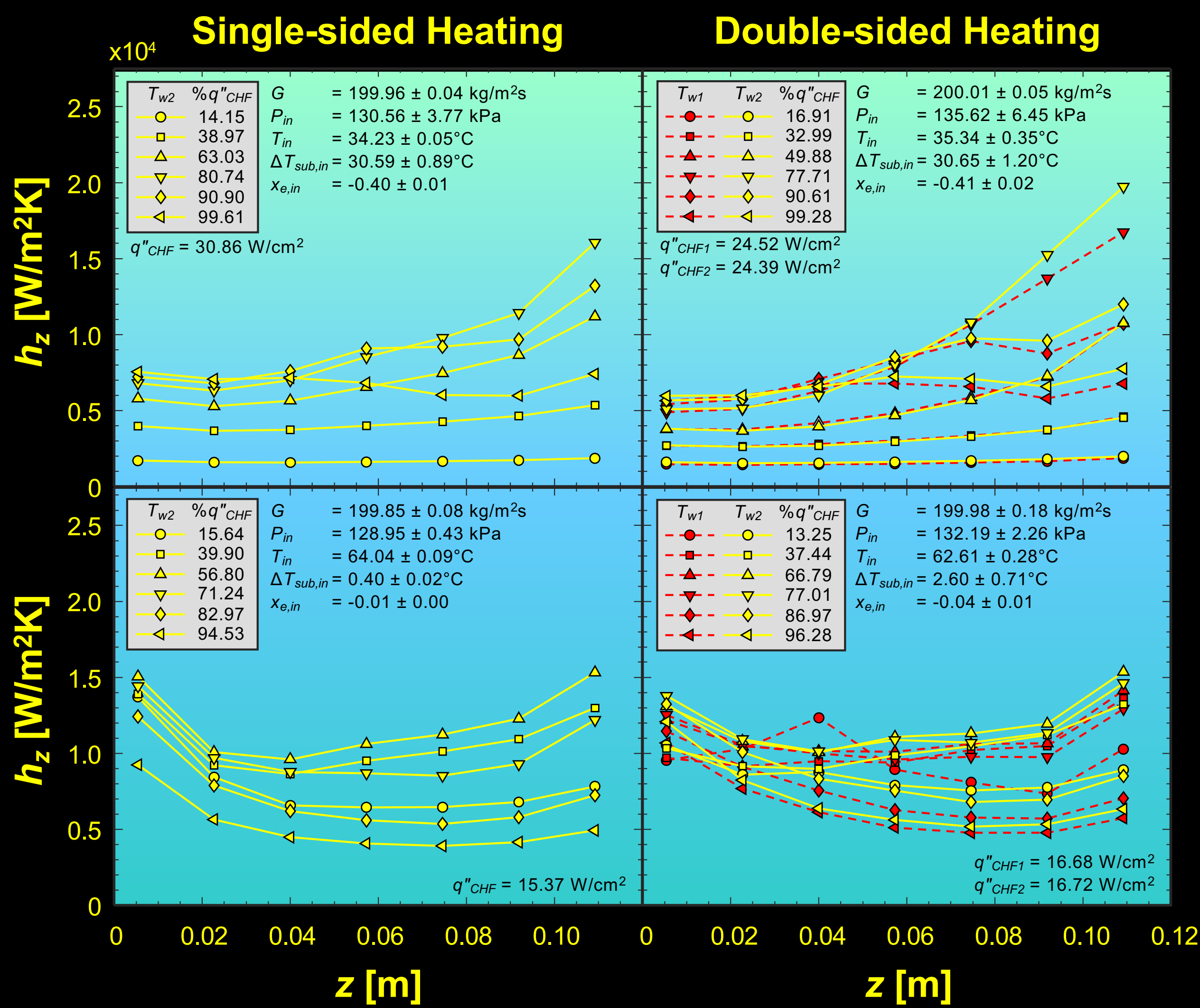

Low Mass Velocity
Highly Subcooled
Low Inlet Pressure

Low Mass Velocity
Near Saturated
Low Inlet Pressure

Average Heat Transfer Coefficient versus Wall Heat Flux

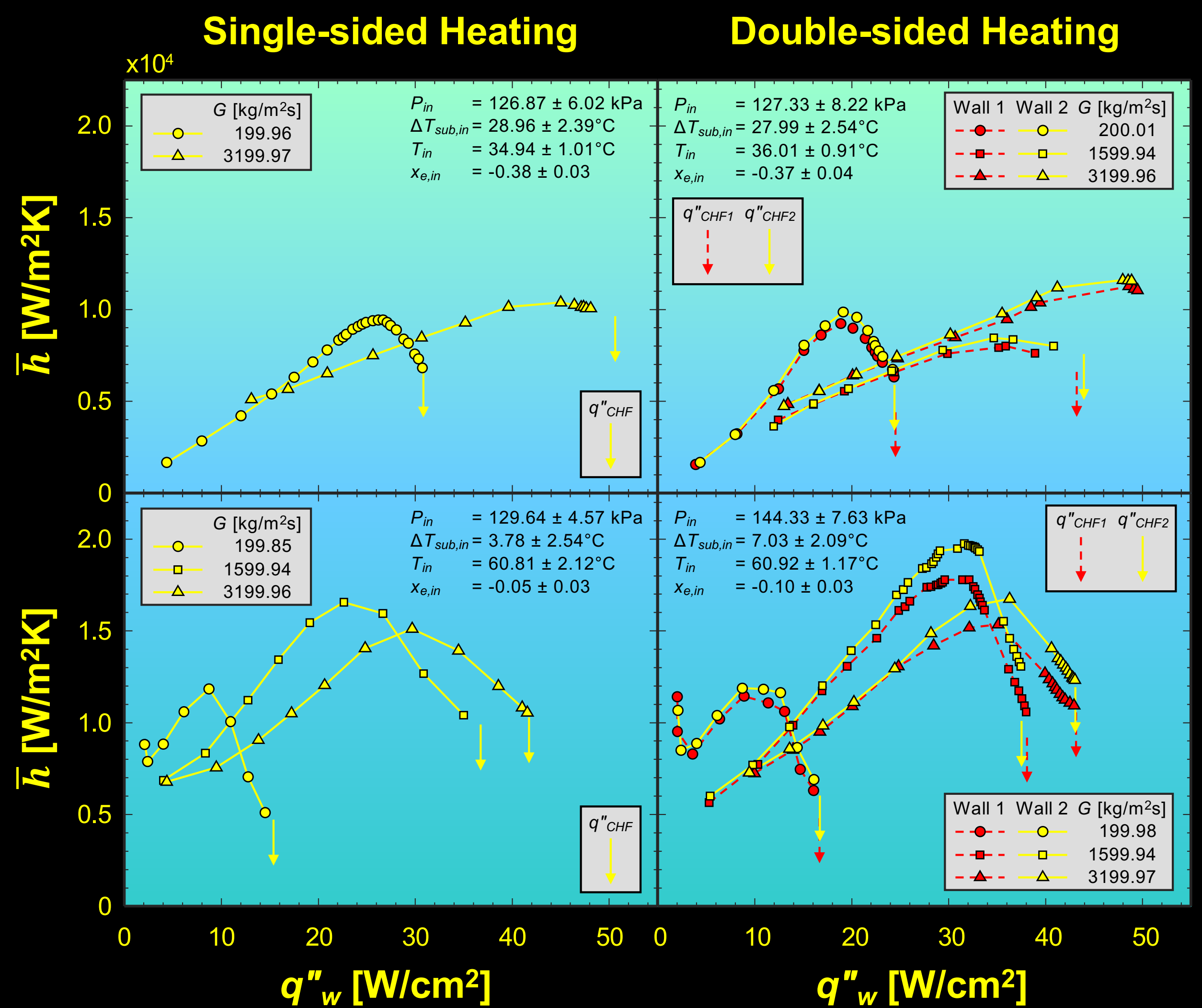

Highly Subcooled
Low Inlet Pressure

Near Saturated
Low Inlet Pressure

Experimental CHF Results - Mission Sequence Testing (MST)

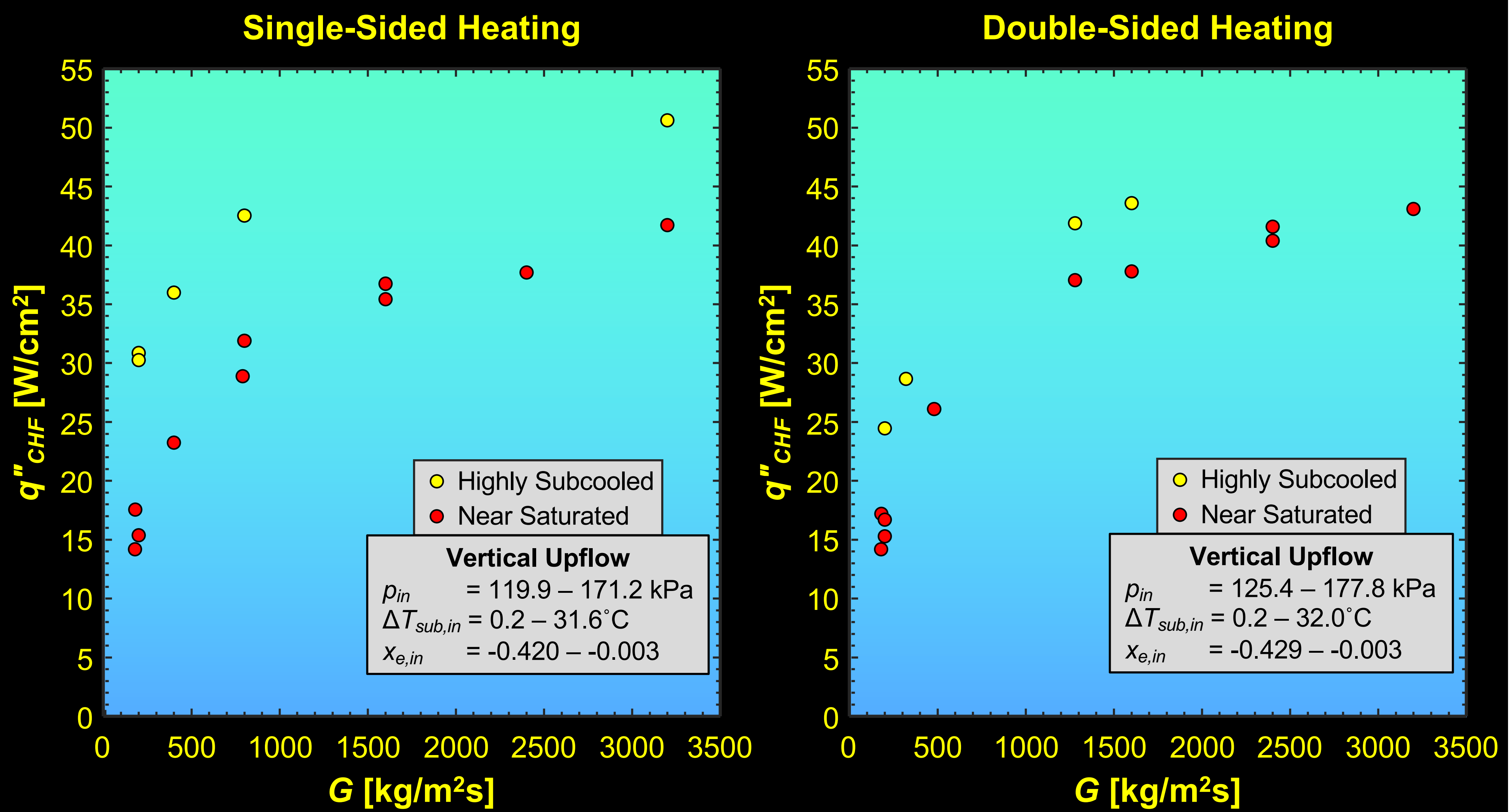

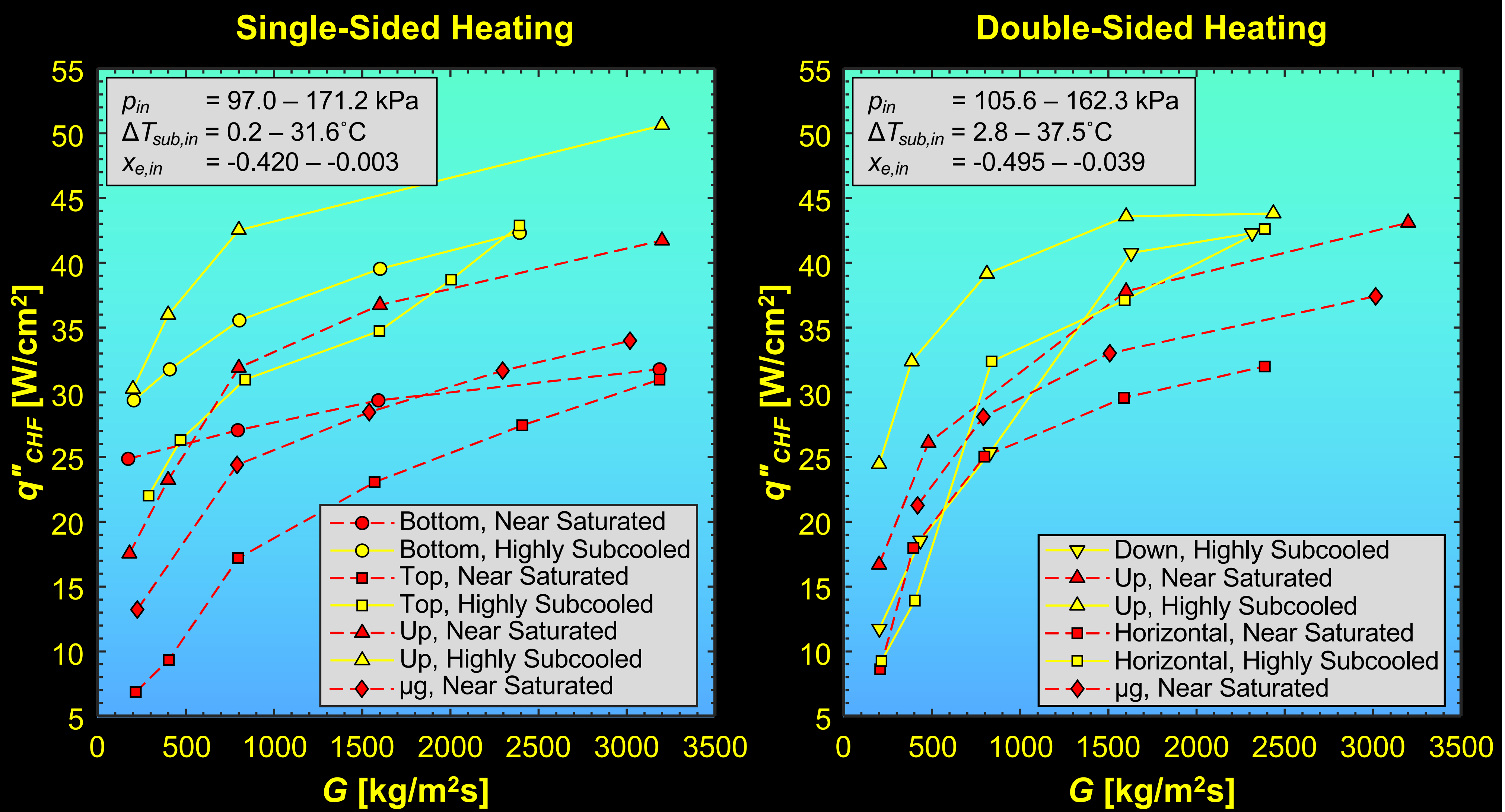
Single-Sided Heating
p_{in} = 97.0 – 171.2 kPa
$\Delta T_{sub,in}$ = 0.2 – 31.6˚C
$x_{e,in}$ = -0.420 – -0.003
Bottom, Near Saturated
Bottom, Highly Subcooled
Top, Near Saturated
Top, Highly Subcooled
Up, Near Saturated
Up, Highly Subcooled
μg, Near Saturated
q"CHF [W/cm²]
G [kg/m²s]
Double-Sided Heating
p_{in} = 105.6 – 162.3 kPa
$\Delta T_{sub,in}$ = 2.8 – 37.5˚C
$x_{e,in}$ = -0.495 – -0.039
Down, Highly Subcooled
Up, Near Saturated
Up, Highly Subcooled
Horizontal, Near Saturated
Horizontal, Highly Subcooled
μg, Near Saturated
q"CHF [W/cm²]
G [kg/m²s]

Flow Visualization – Before and After CHF

Single-Sided Heating

G = 1600 kg/m²s

p_{in} = 130.3 kPa

$\Delta T_{sub,in}$ = 4.6˚C

$x_{e,in}$ = -0.062

q''_{CHF} = 36.74 W/cm²

Pre-CHF Post-CHF

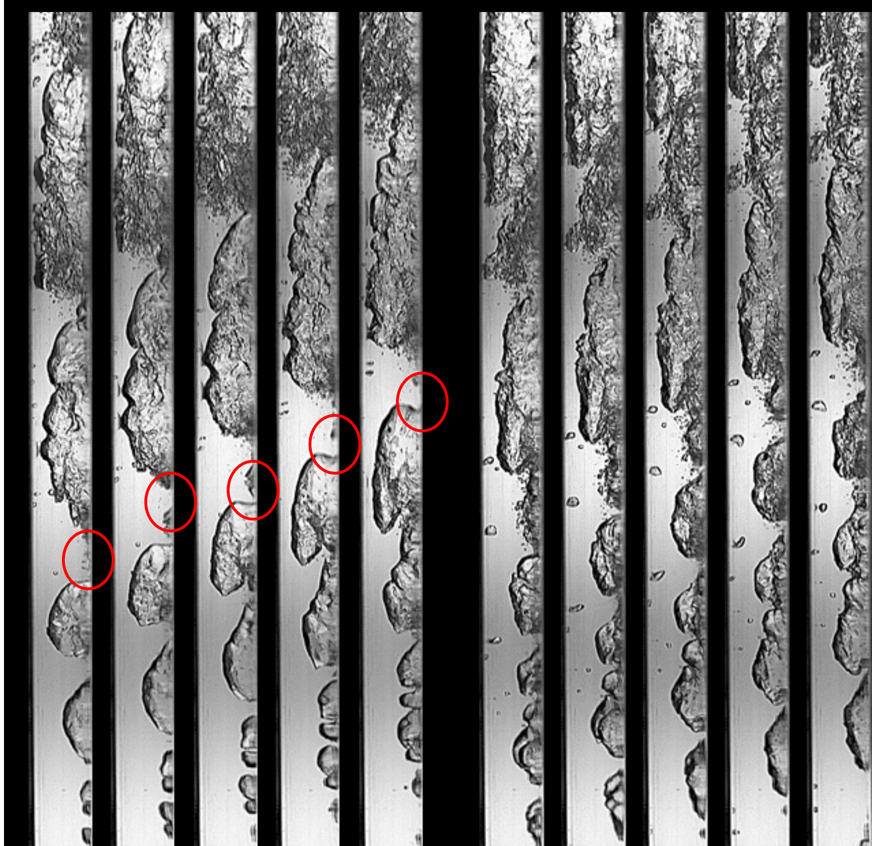

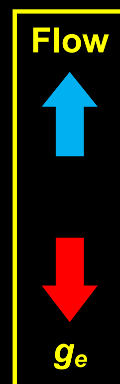

Double-Sided Heating

G = 1600 kg/m²s

p_{in} = 153.3 kPa

$\Delta T_{sub,in}$ = 8.2˚C

$x_{e,in}$ = -0.113

q''_{CHF} = 37.80 W/cm²

Pre-CHF Post-CHF

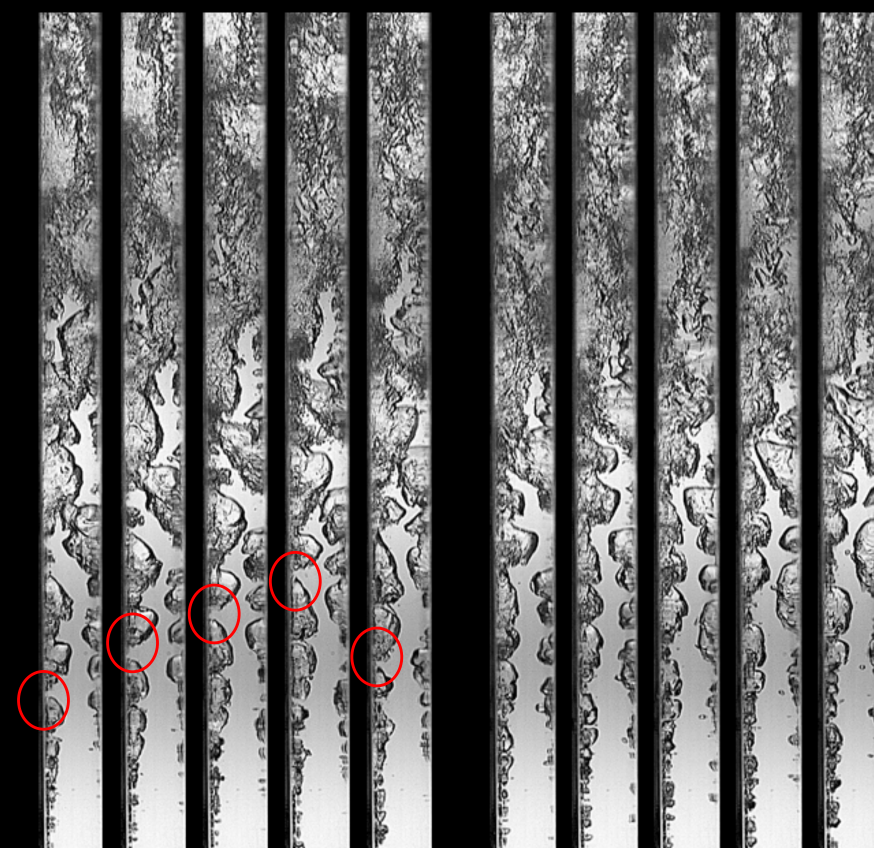

Theoretical & Empirical Analysis

- **Conservation of mass, momentum, and energy utilized to predict axial variations in quality, void fraction, pressure, and fluid properties**
- **One control volume required for liquid layer and one for each vapor layer (depends on number of heated walls)**
- **Heat utility ratio, *ε*, included to account for nonequilibrium effects caused by subcooling**
- **Partitions wall heat flux into fractions dedicated to vaporizing subcooled liquid and to increasing bulk temperature of liquid**

$$\varepsilon = 1 - 0.00285 \frac{\rho_f}{\rho_g} \frac{c_{p,f} \Delta T_{sub,out}}{h_{fg}} \left(\frac{\rho_f U^2 D}{\sigma} \right)$$

$$\frac{dx}{dz} = \frac{\varepsilon q'' W}{GA\left[h_{fg}(z) + \Delta h_{sub} \right]}$$

Single-sided heating

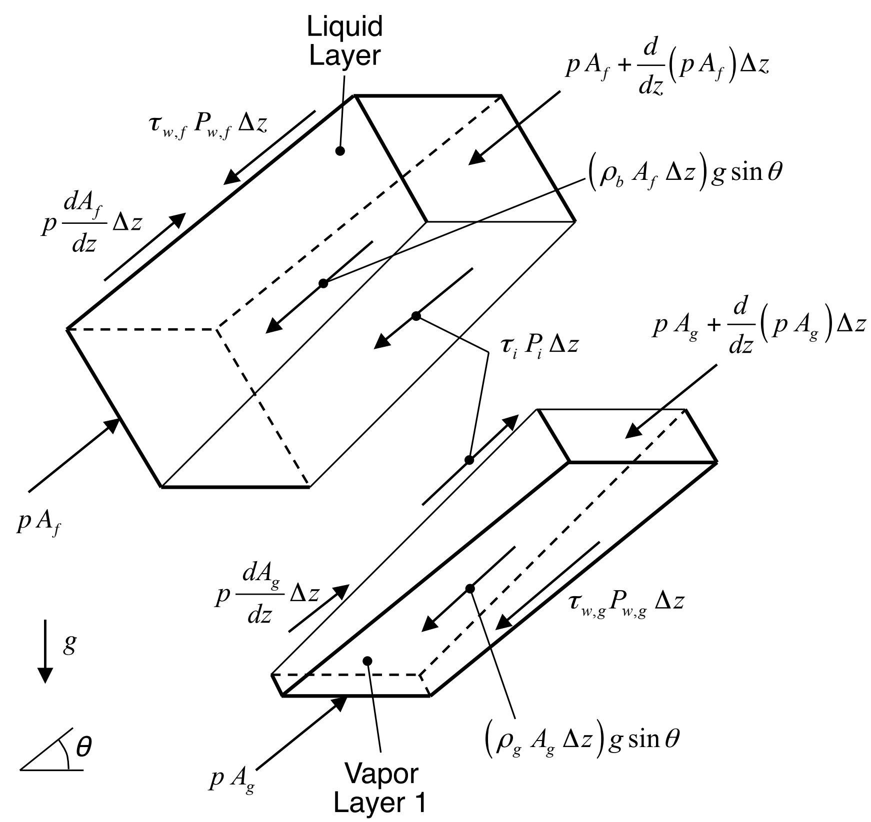

Interfacial Lift-off CHF Model – Instability Analysis, Lift-off Criteria, and Energy Balance

- **Wavy interface is caused by instability between liquid and vapor phases moving at different velocities**
- **Interface described as ideal sinusoid of wavelength λ**
- **Critical wavelength corresponds to neutrally stable interface corresponding to onset of instability**

$$k_c = \frac{2\pi}{\lambda_c} = \frac{\rho''_b \rho''_g (u_g - u_f)^2}{2\sigma(\rho''_b + \rho''_g)} + \sqrt{\left[\frac{\rho''_b \rho''_g (u_g - u_f)^2}{2\sigma(\rho''_b + \rho''_g)}\right]^2 + \frac{(\rho_b - \rho_g) g_n}{\sigma}}$$

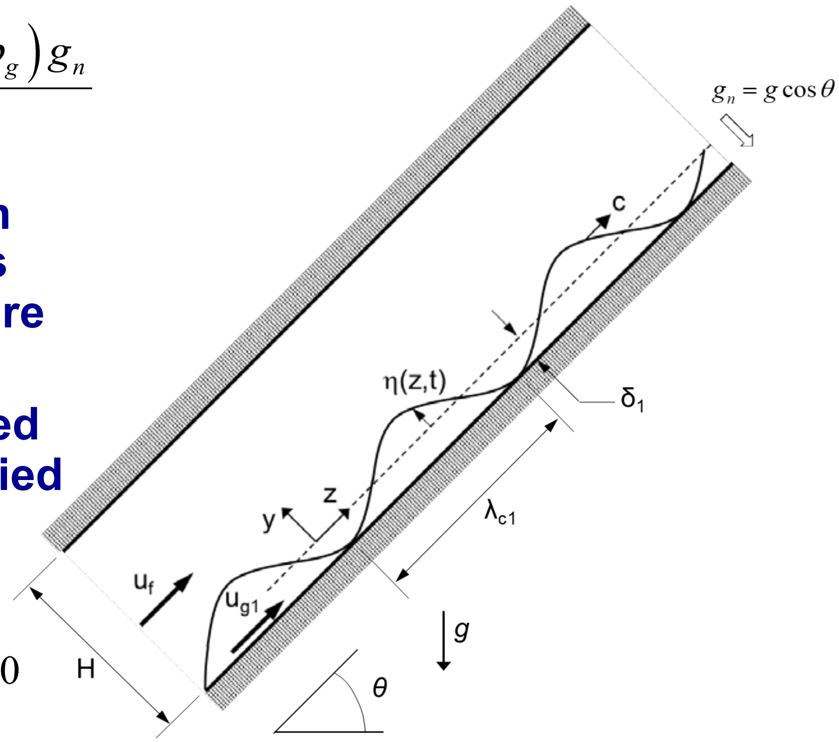

- **CHF occurs when momentum of vapor generated in wetting front, normal to the heated wall, overcomes pressure force corresponding to interfacial curvature that holds wetting front to the wall**
- **Simple energy balance used to relate heat dissipated in wetting fronts that trigger CHF to heat flux supplied to entire wall**

$$q''_{CHF} = \begin{cases} \frac{b}{\varepsilon}\rho_g (c_{p,f}\Delta T_{sub,out} + h_{fg}) \left[\frac{4\pi\sigma b}{\rho_g}\sin(\pi b)\right]^{\frac{1}{2}} \left.\frac{\delta^{1/2}}{\lambda_c}\right|_{z^*}, & x_{e,out} < 0 \\ b\rho_g (c_{p,f}\Delta T_{sub,in} + h_{fg}) \left[\frac{4\pi\sigma b}{\rho_g}\sin(\pi b)\right]^{\frac{1}{2}} \left.\frac{\delta^{1/2}}{\lambda_c}\right|_{z^*}, & x_{e,out} \geq 0 \end{cases}$$

Comparison of Predicted and Measured CHF

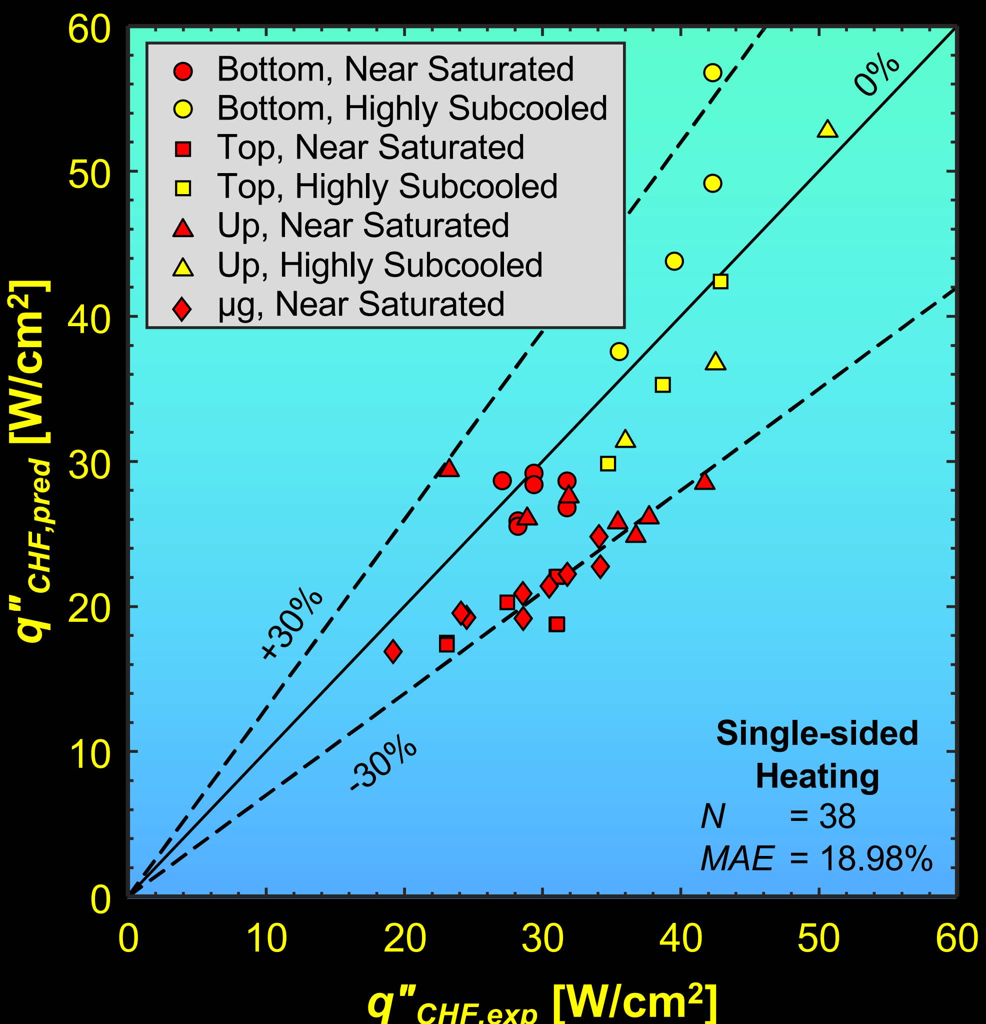

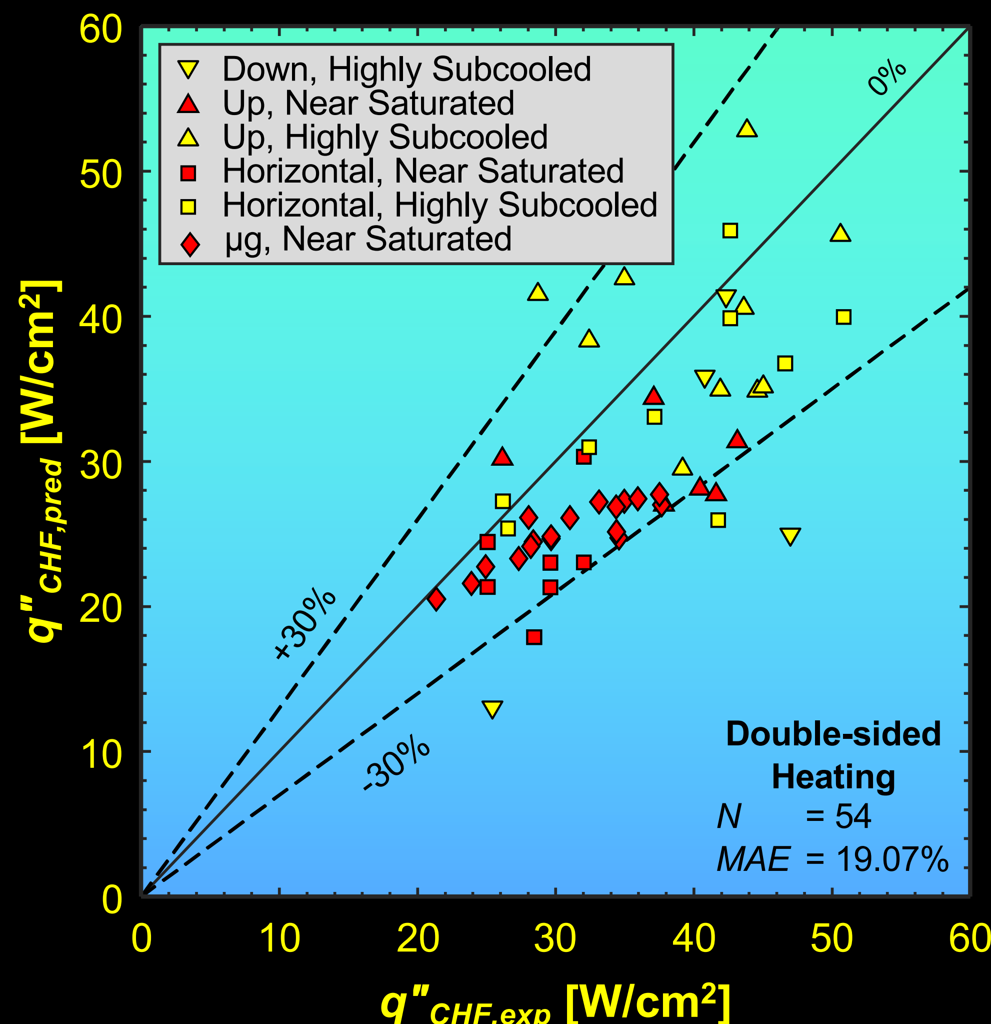

Computational Work

3-D Computational Domain and Mesh Configuration

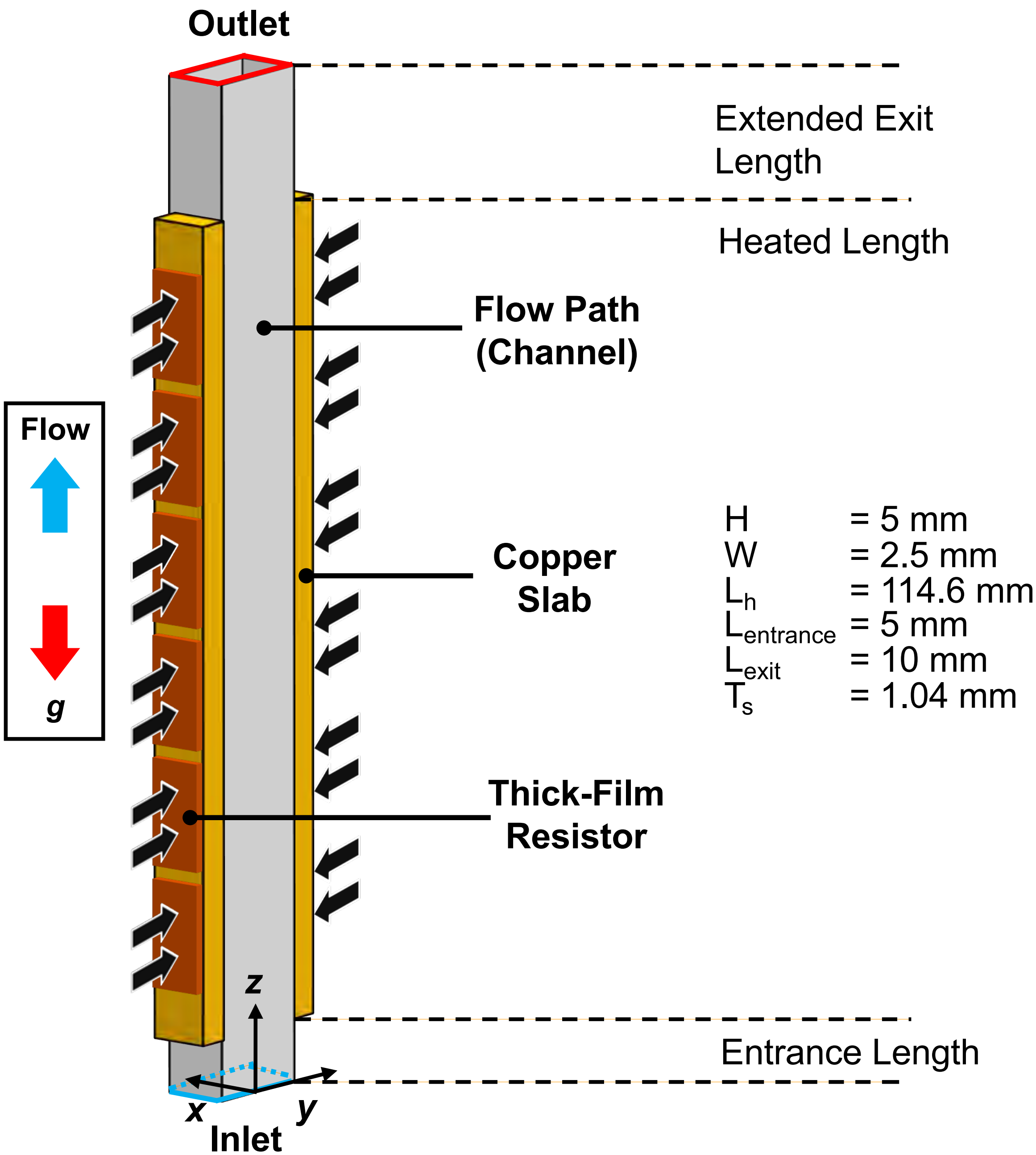

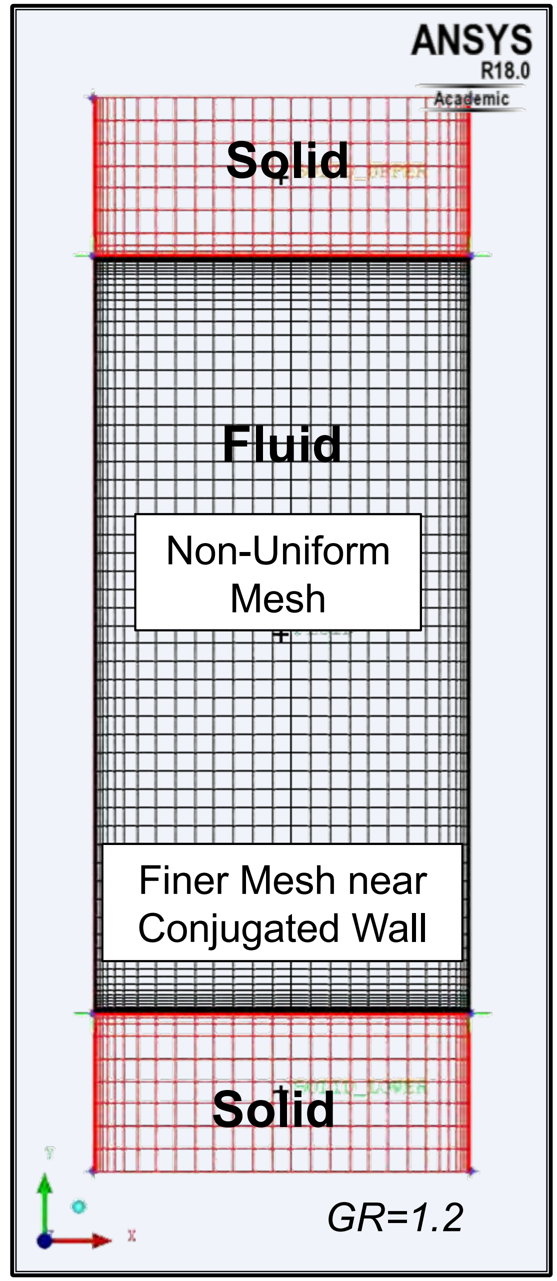

Computational Setup: Boundary and Initial Conditions

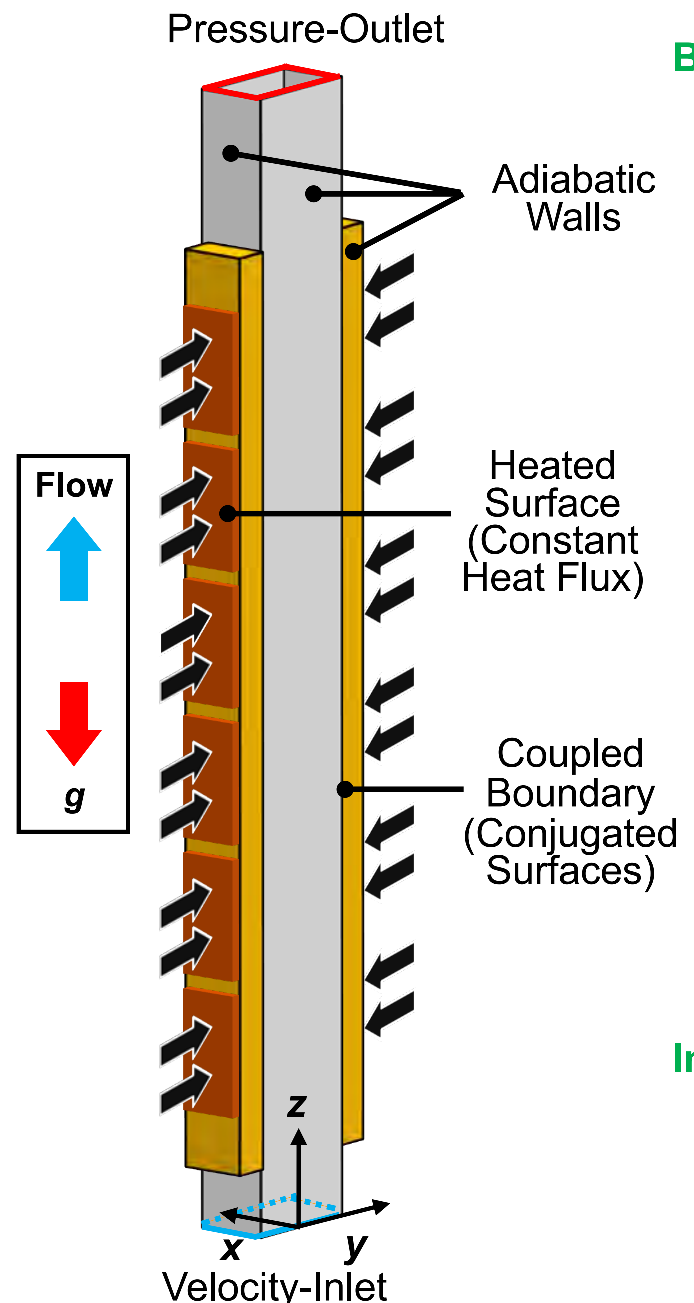

Boundary Conditions

Inlet: Fully developed velocity profile

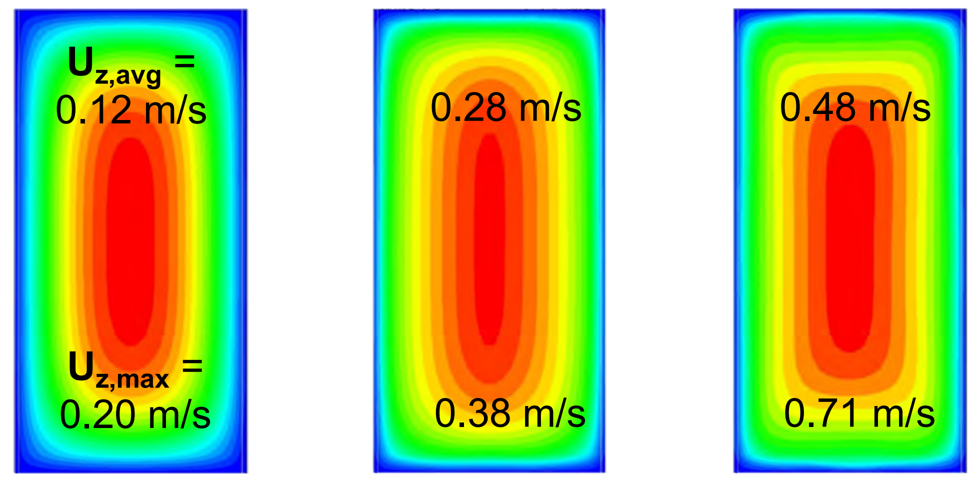

Outlet: Constant pressure
Heated Surface: Constant Heat flux
Conjugated Surface: No slip
Coupled boundary (for thermal energy)
Constant contact angle, 175˚ (for surface tension)
Adiabatic Wall: No slip, zero heat flux
Gravitational Acceleration: $0.05g_e$

Initial Conditions

Velocity field corresponding to the profile of each flow rate
Subcooled liquid only
Turbulence kinetic energy/dissipation rate computed based on 1ϕ flow
Turbulence intensity calculated as $I = 0.16\,\mathrm{Re}^{-1/8}$

Operating Conditions and Thermophysical Properties

- **Operating conditions examined in CFD**

	G [kg/m²s]	u_{avg} [m/s]	q''_w [kW/m²]	% q''_{CHF}	p_{in} [kPa]	$\Delta T_{sub,in}$ [°C]	$x_{e,in}$
CASE 1	200.5	0.12	75.1	37	120.3	5.3	-0.07
CASE 2	444.1	0.28	176.0	69	130.0	7.3	-0.09
CASE 3	758.9	0.48	193.1	67	133.4	5.9	-0.07

- **FC-72 thermophysical properties**

Each property is calculated according to $\phi = \left(1-\alpha_f\right)\phi_f + \alpha_g \phi_g$

G [kg/m²s]	$T_{sat,in}$ [°C]	h_{fg} [J/kg mol]	ρ_f [kg/m³]	$c_{p,f}$ [J/kg·K]	k_f [W/m·K]	μ_f [kg/m·s]	ρ_g [kg/m³]	$c_{p,g}$ [J/kg·K]	k_g [W/m·K]	μ_g [kg/m·s]	σ [N/m]
200.5	62.1	2.773×10^{7}	1608.8	1117.5	0.0536	3.848×10^{-4}	15.966	942.70	0.0142	1.210×10^{-5}	0.0080
444.1	64.4	2.749×10^{7}	1602.4	1122.4	0.0533	3.731×10^{-4}	17.164	950.69	0.0144	1.220×10^{-5}	0.0078
758.9	62.9	2.750×10^{7}	1602.4	1122.4	0.0533	3.732×10^{-4}	17.157	950.65	0.0144	1.220×10^{-5}	0.0080

Computational Methodology

Computational Models used:

- **Volume-of-Fluid (VOF) Model**
  tracks interface between liquid and vapor, involving interface shape reconstruction
- **Shear-Stress Transport (SST) k-ω Model**
  accounts for turbulence effects including interfacial damping
- **Lee Model**
  predicts interfacial mass and heat transfer resulting from phase change, evaporation and condensation
- **Continuum Surface Force (CSF) Model**
  adds surface tension to the VOF calculation, considering the pressure jump across the surface

Governing Equations:

- **Continuity of Volume Fraction**

$$\frac{\partial \alpha_f}{\partial t} + \nabla \bullet \left(\alpha_f \vec{u}_f \right) = \frac{1}{\rho_f} \sum \left(\dot{m}_{gf} - \dot{m}_{fg} \right)$$

$$\frac{\partial \alpha_g}{\partial t} + \nabla \bullet \left(\alpha_g \vec{u}_g \right) = \frac{1}{\rho_g} \sum \left(\dot{m}_{fg} - \dot{m}_{gf} \right)$$

- **Momentum**

$$\frac{\partial}{\partial t}\left(\rho \vec{u} \right) + \nabla \bullet \left(\rho \vec{u}\vec{u} \right) = -\nabla P + \nabla \bullet \left[\mu \left(\nabla \vec{u} + \nabla \vec{u}^T \right) \right] + \vec{F}$$

- **Energy**

$$\frac{\partial}{\partial t}\left(\rho E \right) + \nabla \bullet \left(\vec{u} \left(\rho E + P \right) \right) = \nabla \bullet \left(k_{eff} \nabla T \right) + S_h$$

- **Turbulent Kinetic Energy and Dissipation Transport**

$$\frac{\partial}{\partial t}\left(\rho k \right) + \nabla \bullet \left(\rho k \vec{u} \right) = \nabla \bullet \left(\Gamma_k \nabla k \right) + \widetilde{G_k} - Y_k + S_k$$

$$\frac{\partial}{\partial t}\left(\rho \omega \right) + \nabla \bullet \left(\rho \omega \vec{u} \right) = \nabla \bullet \left(\Gamma_\omega \nabla \omega \right) + G_\omega - Y_\omega + D_\omega + S_\omega$$

Limitation of Volume-of-Fluid Method

G = 836.64–833.14 kg/m²s
q''_w = 19.1–24.6 W/cm²
$\Delta T_{sub,in}$ = 30.81–31.24°C

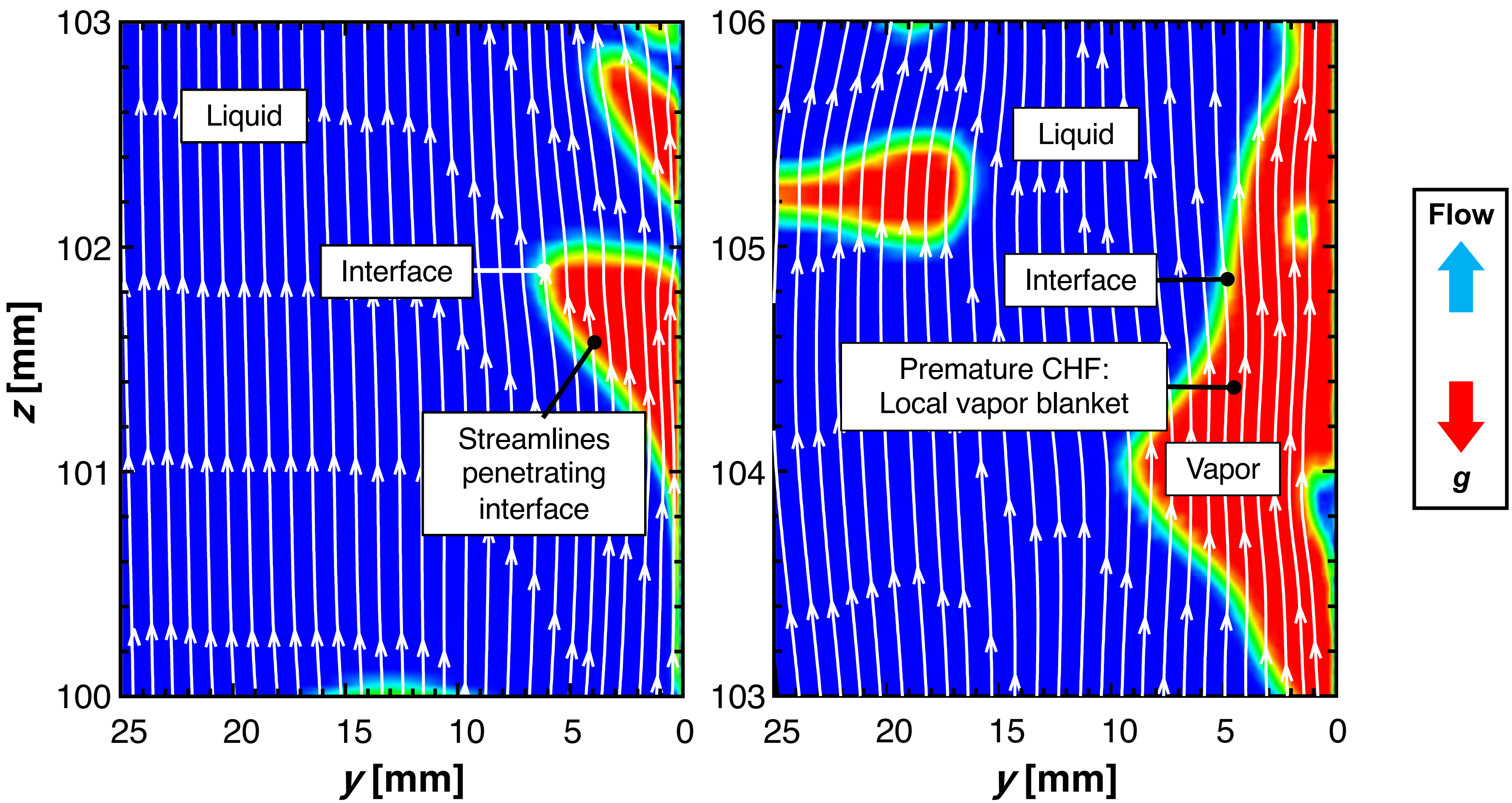

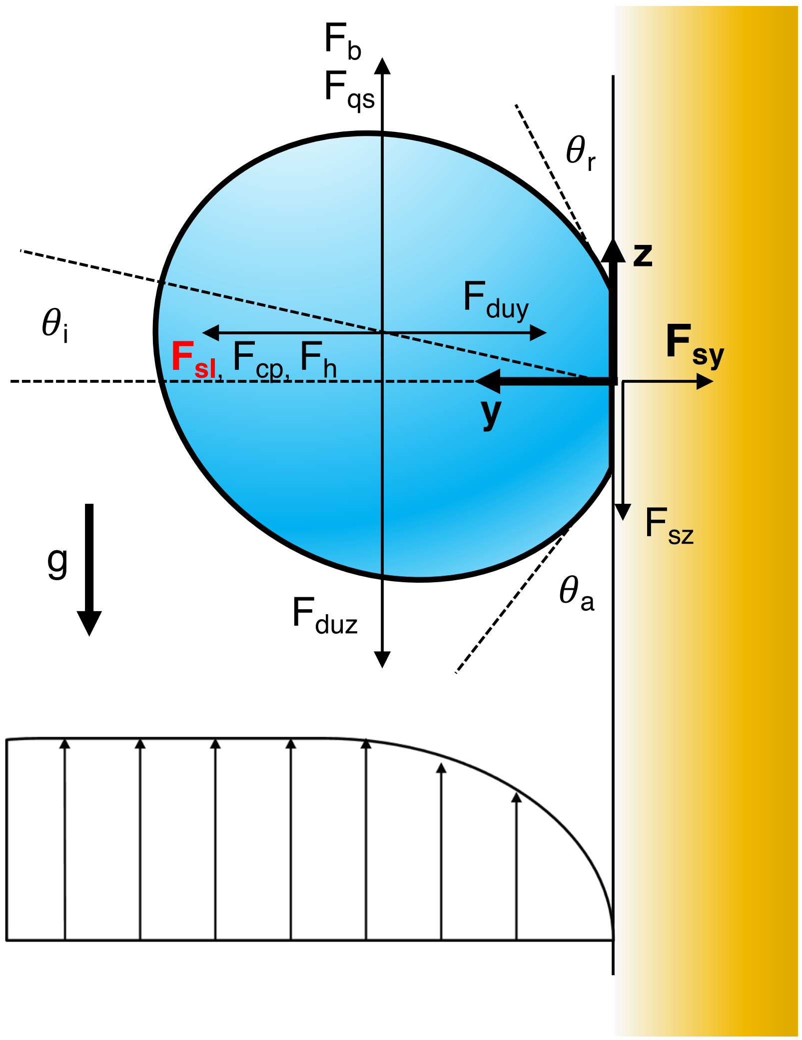

Forces parallel to surface

$$\sum F_z = F_{s,z} + F_{du,z} + F_{qs} + F_b = \rho_g V_b \frac{du_z}{dt}$$

Forces normal to surface

$$\sum F_y = F_{s,y} + F_{du,y} + F_{sl} + F_h + F_{cp} = \rho_g V_b \frac{du_y}{dt}$$

Shear-lift coefficient

$$C_L = \frac{F_{sl}}{\frac{1}{2}\rho_f U_r^2 \pi a^2} = 3.877 G_s^{1/2} \times \left[\mathrm{Re}_b^{-m/2} + \left(0.344 G_s^{1/2}\right)^m \right]^{1/m}$$

m=4

Dimensionless shear rate

$$G_s = \left|\frac{dU_r}{dy}\right| \frac{a}{U_r} \quad , a=d_b/2$$

Comparison of CFD and Flow Visualization Results

p_{in} = 120.3 kPa
G = 200.5 kg/m²s
q''_w = 7.517 W/cm²
$x_{e,in}$ = -0.07

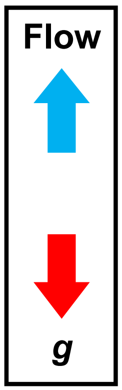

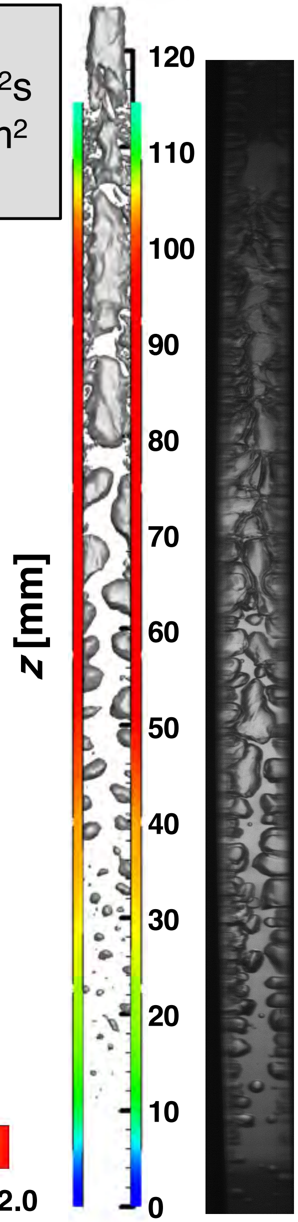

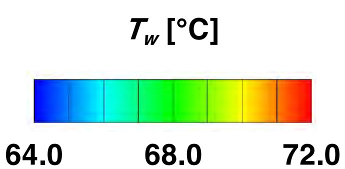

p_{in} = 130.0 kPa
G = 444.1 kg/m²s
q''_w = 17.604 W/cm²
$x_{e,in}$ = -0.09

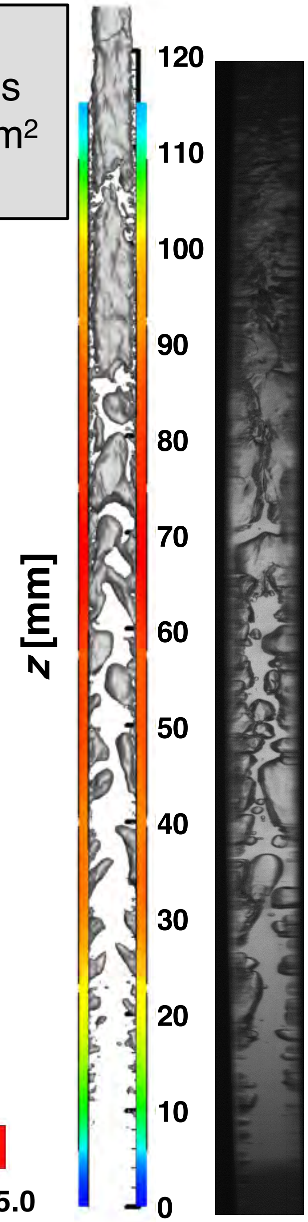

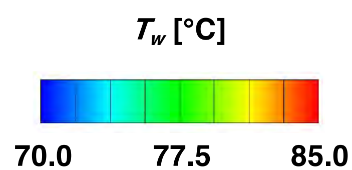

p_{in} = 133.4 kPa
G = 758.9 kg/m²s
q''_w = 19.316 W/cm²
$x_{e,in}$ = -0.07

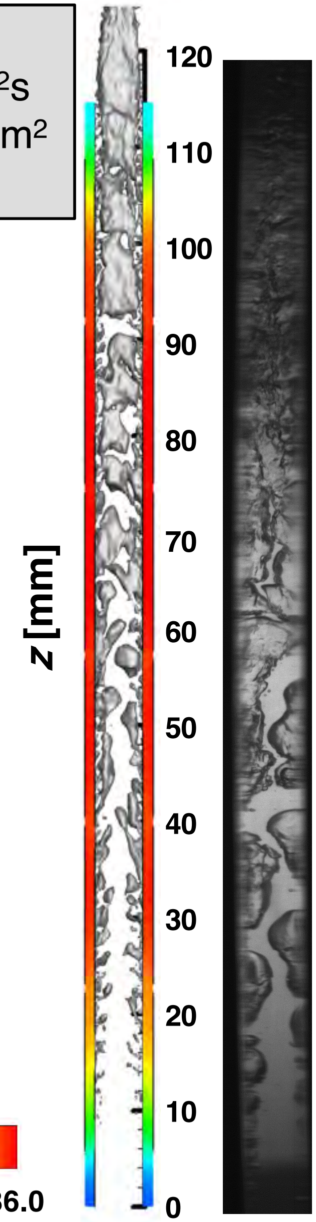

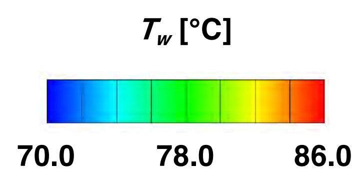

Details of Predicted Bubble Motion

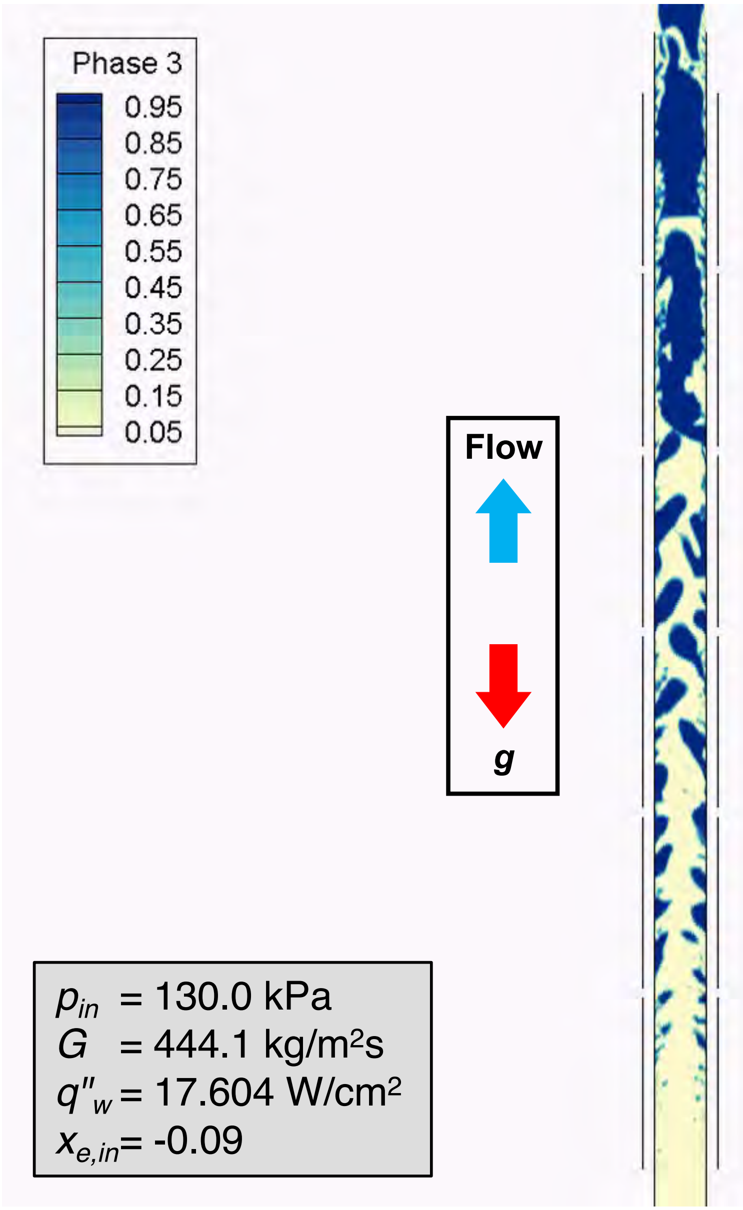

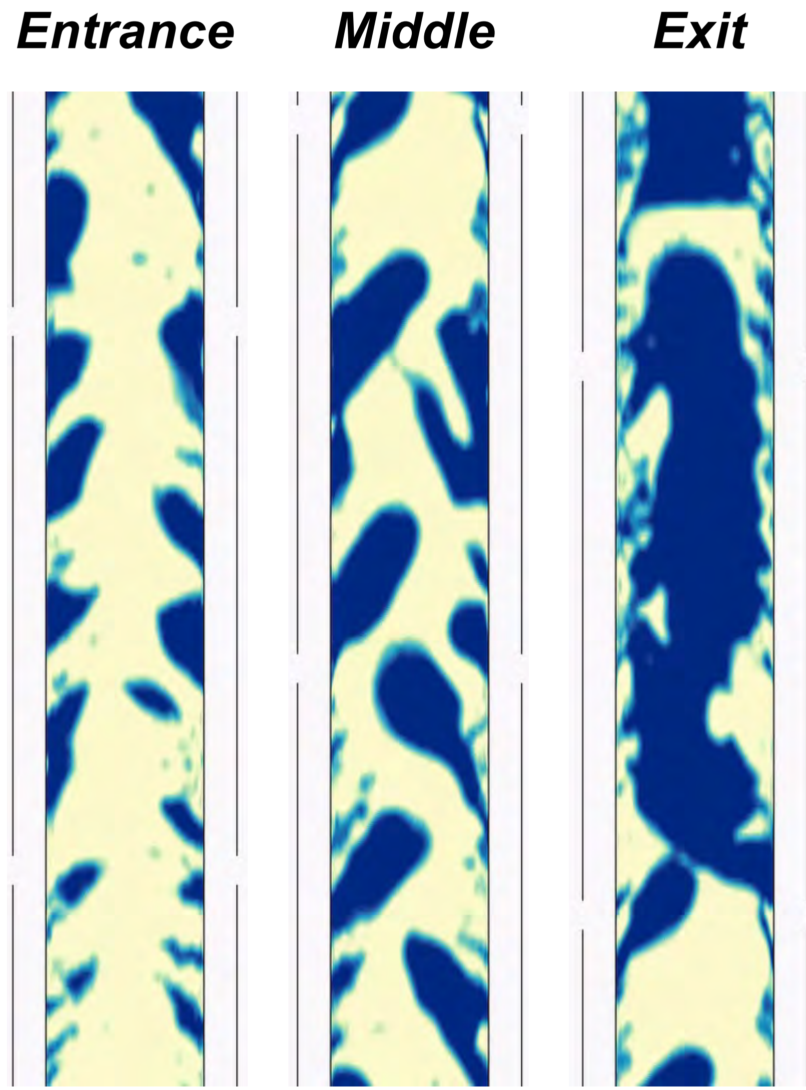

Vapor Formation in Cross-Section at Different Axial Locations

p_{in} = 120.3 kPa
G = 200.5 kg/m²s
q''_w = 7.517 W/cm²
$x_{e,in}$ = -0.07

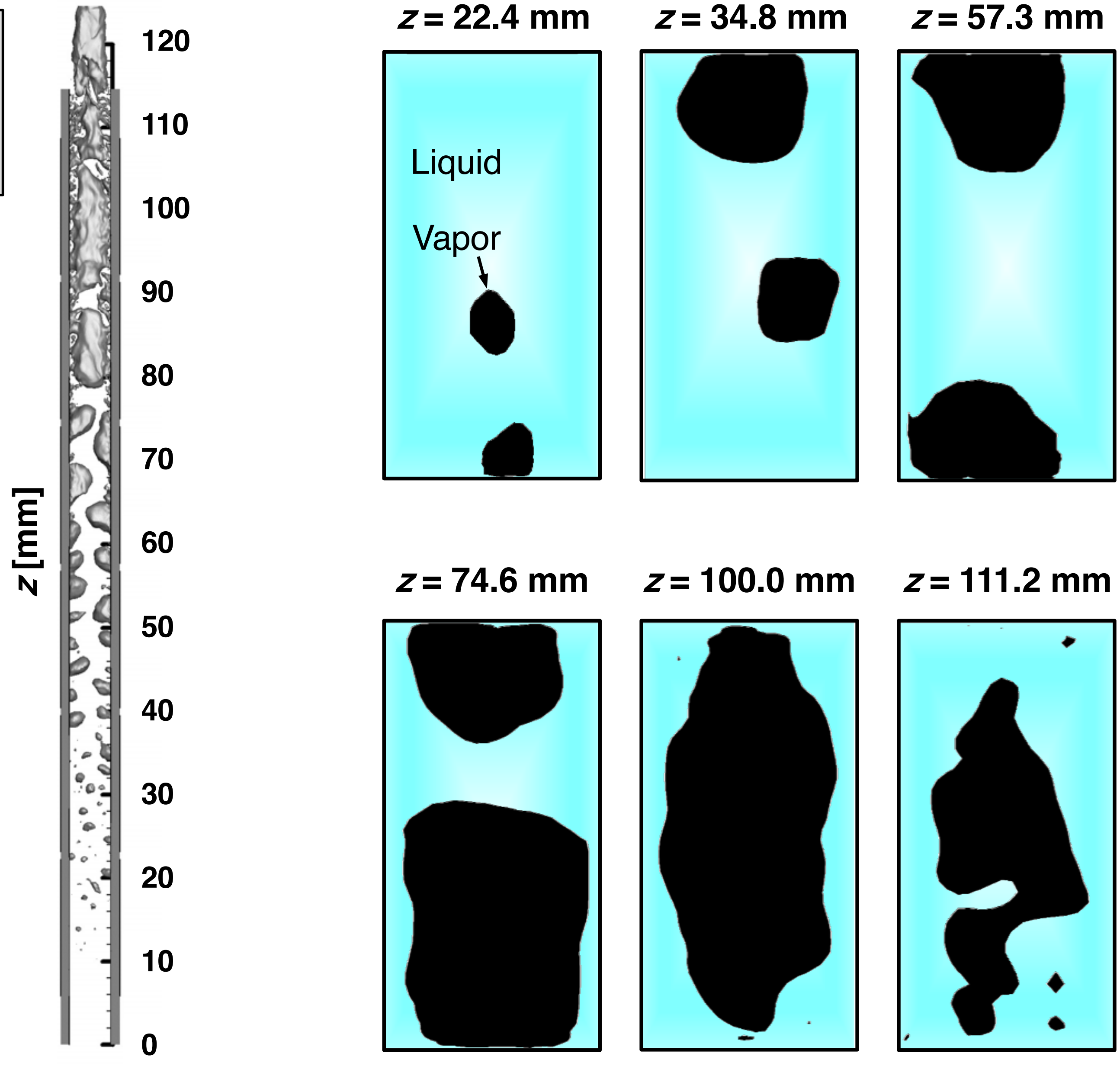

Vapor Formations in Cross-Section at Different Axial Locations

p_{in} = 130.0 kPa
G = 444.1 kg/m^{2}s
q''_w = 17.604 W/cm^2
$x_{e,in}$ = -0.09

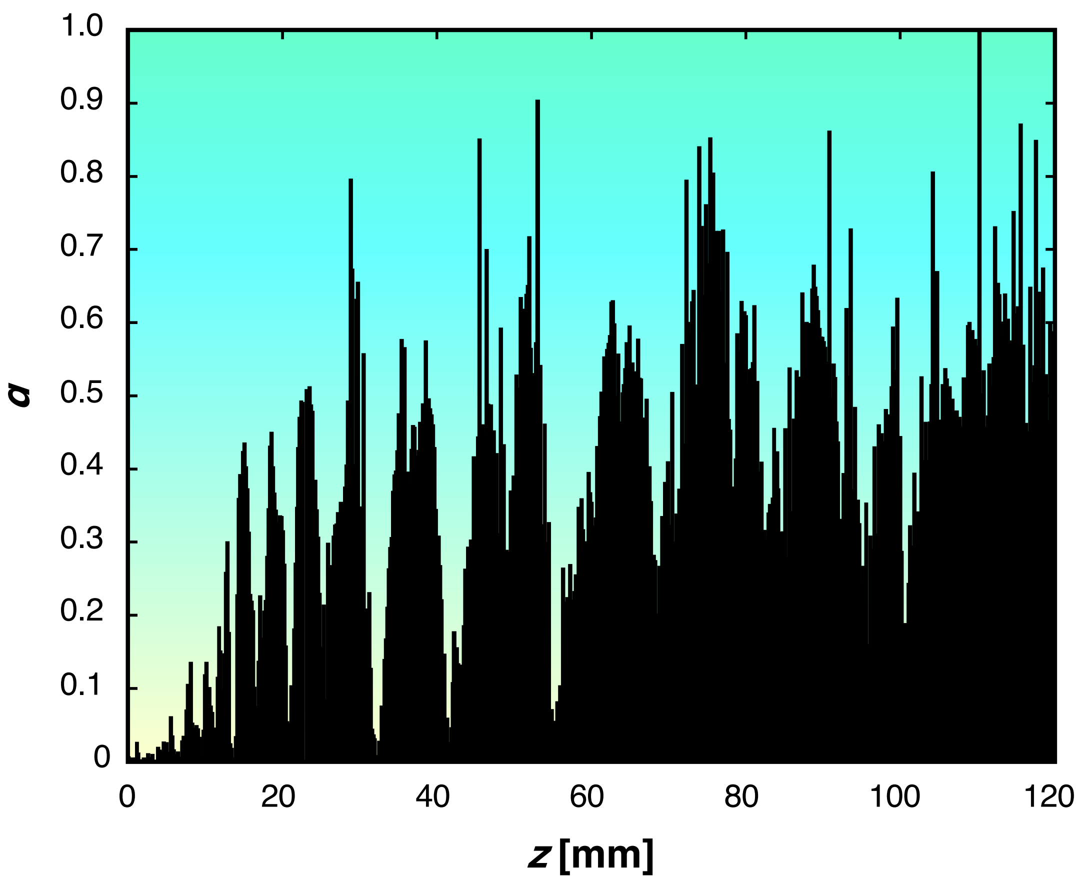

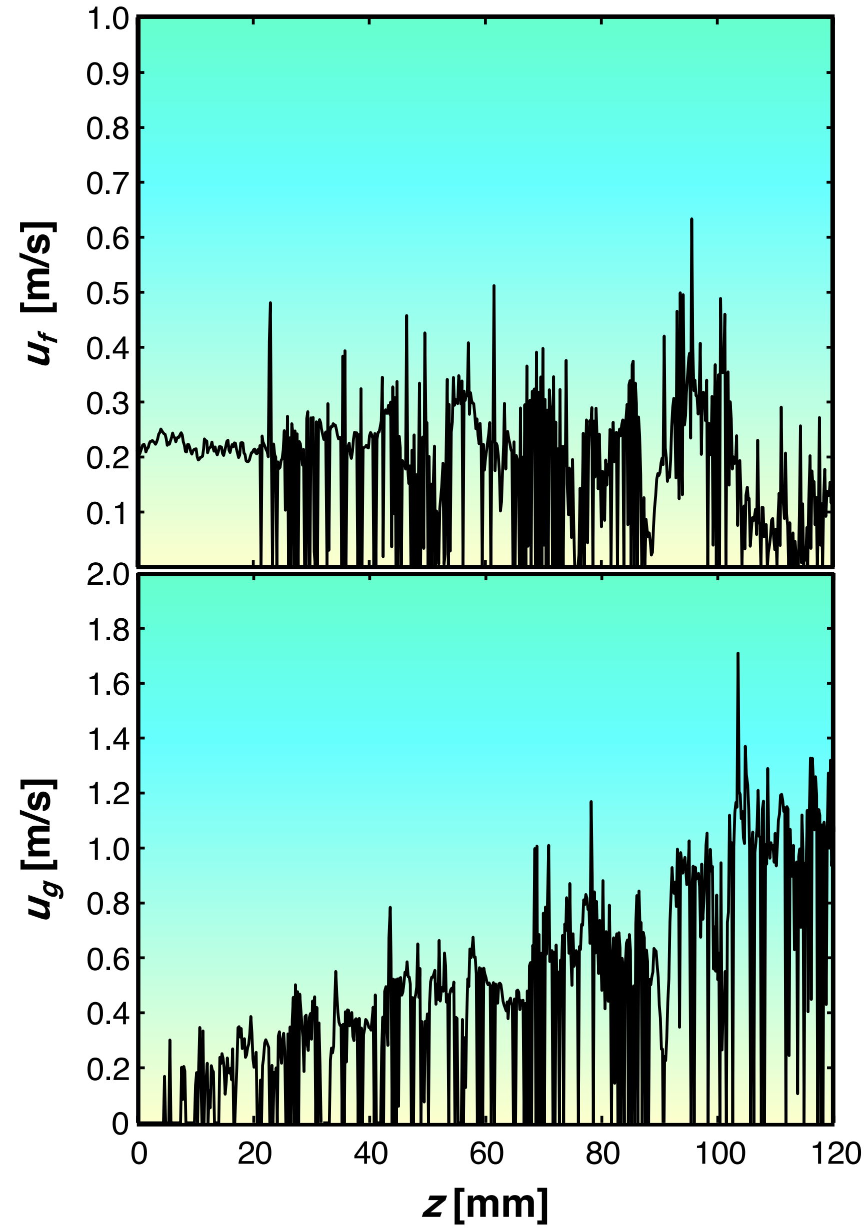

Computed Two-Phase Structure in One g_e versus Low g

1 g_e	0.05 g_e
p_{in} = 124.5 kPa G = 445.7 kg/m²s q''_w = 27.871 W/cm² (78% q''_{CHF})	p_{in} = 130.0 kPa G = 444.1 kg/m²s q''_w = 17.604 W/cm² (69% q''_{CHF})

Entrance

1 g_e 0.05 g_e

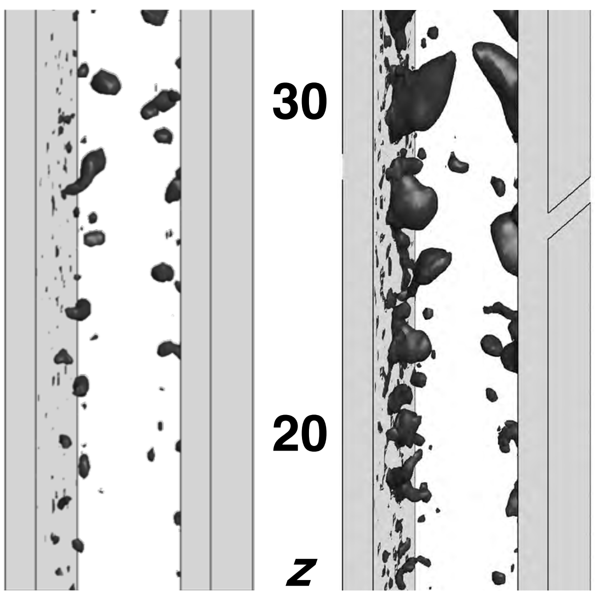

Middle

1 g_e 0.05 g_e

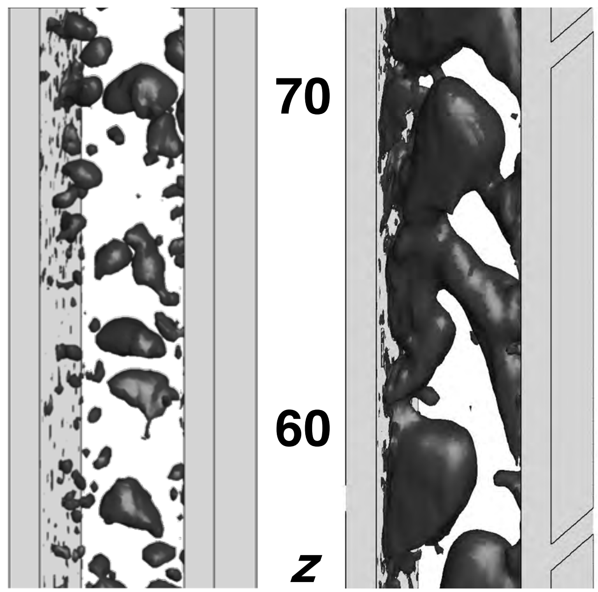

Exit

1 g_e 0.05 g_e

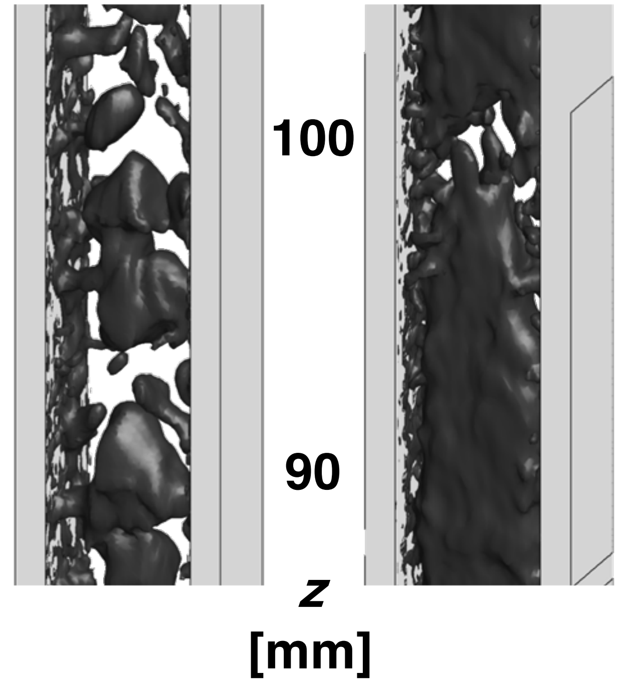

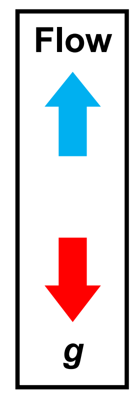

Comparison of Predicted and Measured Wall Temperatures

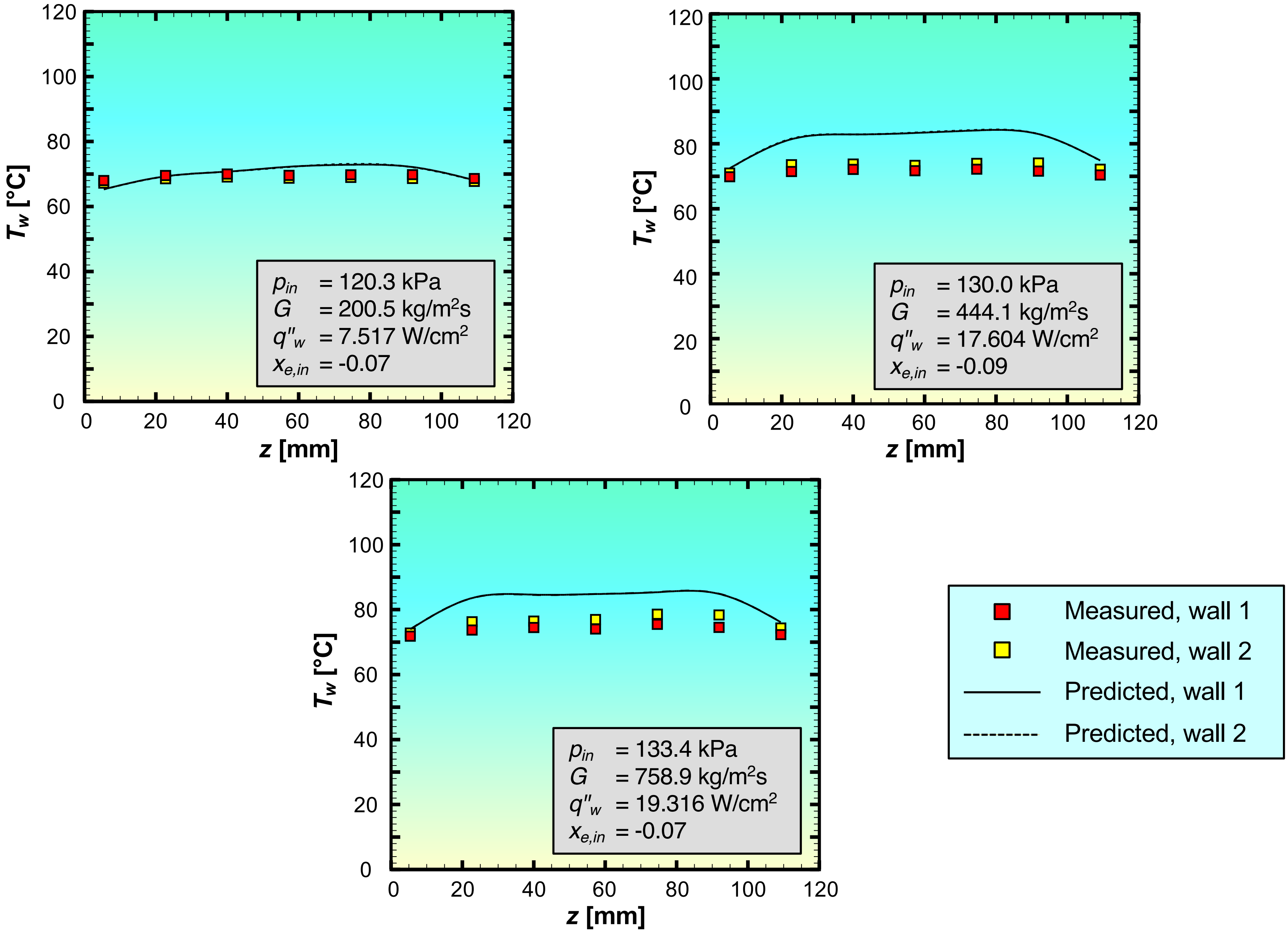

Time-Averaged Transverse Void Fraction and Stream-Wise Velocity Profiles

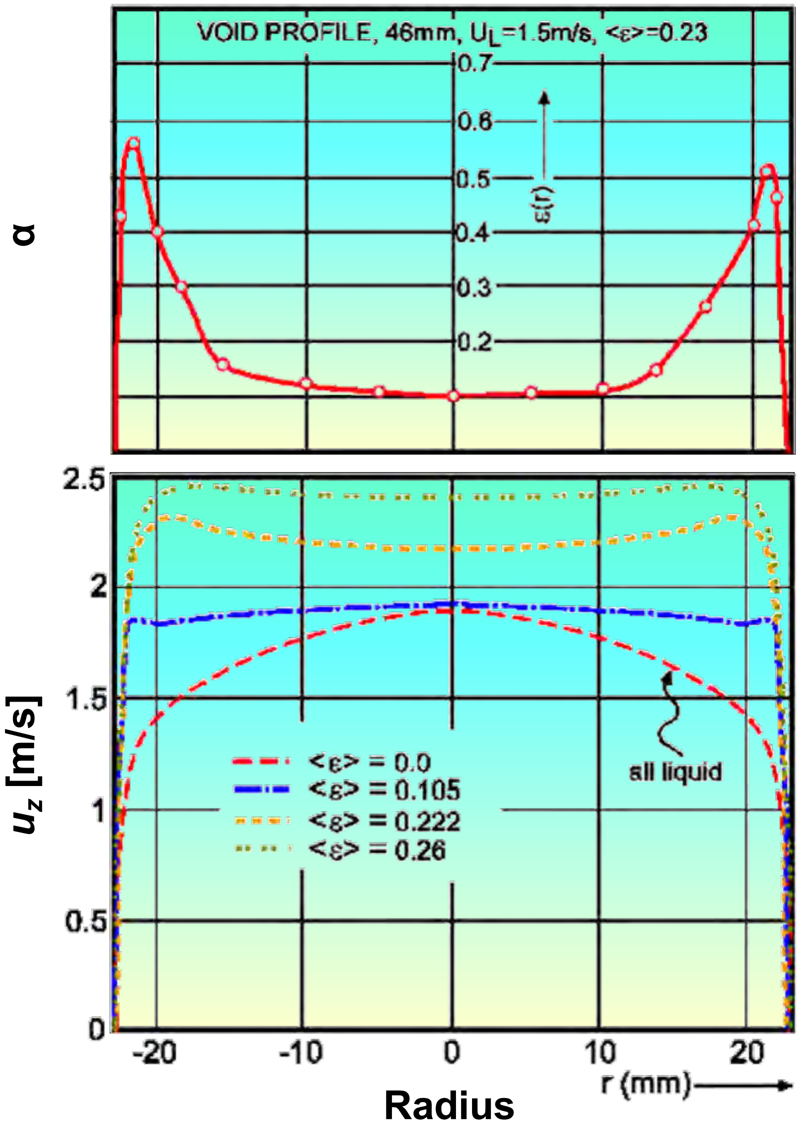

Radial void fraction and velocity profiles for air-water measured by Malnes (1966)

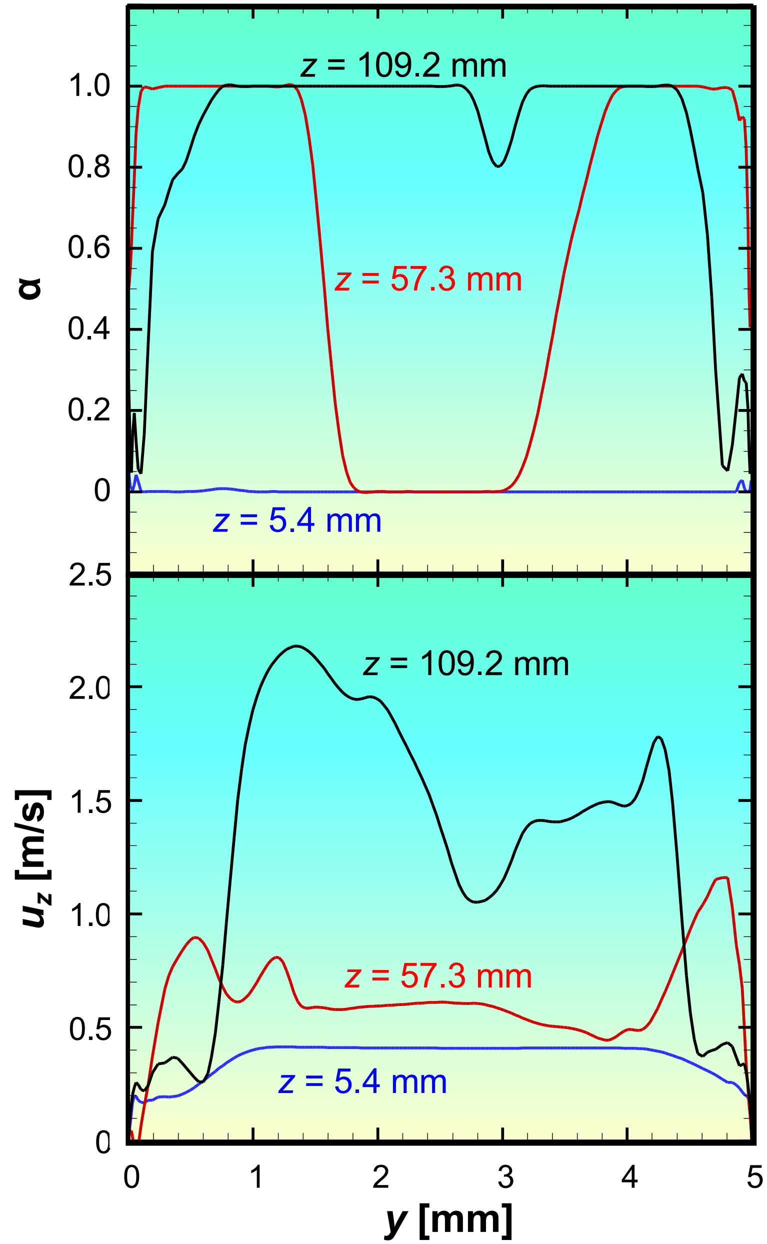

Thank you!

Supplementary Material

Parameter ranges included in predictions

Configuration	G [kg/m²s]	p_{in} [kPa]	T_{in} [˚C]	$\Delta T_{sub,in}$ [˚C]	$x_{e,in}$	Orientation	Limitation
Single	794 – 3199	99.0 – 161.8	29.9 – 66.9	3.9 – 28.3	-0.362 – -0.054	Horizontal Bottom	$u_{in} > 0.5$ m/s
Single	1570 – 3200	100.1 – 161.5	29.8 – 67.2	3.6 – 28.4	-0.363 – -0.048	Horizontal Top	$u_{in} > 0.15$ m/s
Single	400 – 3200	119.9 – 171.2	36.6 – 71.6	0.5 – 28.0	-0.380 – -0.007	Up	$u_{in} > 0.15$ m/s
Single (µg)	420 – 3019	122.4 – 150.0	58.8 – 63.4	3.6 – 5.9	-0.081 – -0.049	Up	$u_{in} > 0.15$ m/s
Double	793 – 2409	100.2 – 165.8	27.6 – 64.7	4.9 – 33.2	-0.435 – -0.065	Horizontal	$u_{in} > 0.5$ m/s
Double	320 – 3200	125.4 – 190.8	28.9 – 73.0	3.7 – 35.4	-0.467 – -0.051	Up	$u_{in} > 0.15$ m/s
Double	831 – 2314	130.6 – 179.7	27.9 – 51.6	23.6 – 37.5	-0.495 – -0.330	Down	$u_{in} > 0.5$ m/s
Double (µg)	391 – 3050	109.8 – 166.8	51.0 – 65.5	1.9 – 9.6	-0.125 – -0.025	Up	$u_{in} > 0.15$ m/s

Computed Two-Phase Structure in g_e versus Reduced g